

356001  
MORNING  
070778

STUDIES OF RADIO-FREQUENCY GAS DISCHARGES

PART I: The Impedance of an R.F. Discharge

PART II: A Spectroscopic Study of the  
Temperatures of an R.F. Discharge

\*\*\*\*\*

- by -

N.A. Surplice.

Department of Electron Physics

University of Birmingham

1955

In supplication for the degree of Ph.D

UNIVERSITY OF  
BIRMINGHAM

**University of Birmingham Research Archive**

**e-theses repository**

This unpublished thesis/dissertation is copyright of the author and/or third parties. The intellectual property rights of the author or third parties in respect of this work are as defined by The Copyright Designs and Patents Act 1988 or as modified by any successor legislation.

Any use made of information contained in this thesis/dissertation must be in accordance with that legislation and must be properly acknowledged. Further distribution or reproduction in any format is prohibited without the permission of the copyright holder.

CONTENTS

Page.

SUMMARY.

1

ACKNOWLEDGMENTS.

- (1) REVIEW OF PREVIOUS WORK. 3
- (2) BASIC DIFFERENCES BETWEEN D.C. AND R.F. DISCHARGES. 13

The author thanks the following for their help:

- (4b) DESIGN OF NEW APPARATUS. 22

Professor J.Sayers for his continual guidance and encouragement throughout these studies.

- (5) TESTING OF APPARATUS. 26

Members of the Electron Physics Department for discussions, particularly Dr.K.W.Champion for those on Part I and Mr.F.J.Bryant for those on Part II of the work.

- (7) METHODS OF MEASURING THE TEMPERATURES OF

The Department of Scientific and Industrial Research for the award of a maintenance allowance from 1951 to 1954.

- (7.2) Examination temperature. 36

- (7.5) Equilibrium temperature. 41

- (7.6) Comparison of \*\*\*\*\* methods with the same discharge. 43

- (8) MEASUREMENT OF AVERAGE IONIC TEMPERATURES FROM THE DOPPLER BROADENING OF SPECTRUM LINES. 45

- (8.1) Doppler broadening. 45

- (8.2) Other causes of line broadening. 45

- (9) REVIEW OF PREVIOUS METHODS OF MEASUREMENT OF TEMPERATURE FROM THE DOPPLER BROADENING OF SPECTRUM LINES. 48

- (10) THE CHOICE OF EXPERIMENTAL CONDITIONS. 54

- (10.1) Spectrum lines. 54

- (10.2) Discharge pressure. 56

- (10.3) Power Supply. 56

- (11) PRELIMINARY EXPERIMENTS WITH PULSED D.C. DISCHARGES. 58

- (12) APPARATUS FOR EXPERIMENTS WITH R.F. DISCHARGES. 59

- (12.1) Arrangement of apparatus. 59

- (12.2) The oscillator. 59

- (12.3) The gas circulating system. 59

- (12.4) Spectroscopic apparatus. 59

- (12.5) Discharge tubes. 59

## CONTENTS

	<u>Page.</u>
SUMMARY.	1
 <u>PART I.</u> 	
(1) REVIEW OF PREVIOUS WORK	3
(2) BASIC DIFFERENCES BETWEEN D.C. AND R.F. DISCHARGES.	13
(3) THE PROGRAMME OF RESEARCH.	18
(4a) APPARATUS PROVIDED	21
(4b) DESIGN OF NEW APPARATUS	22
(4.1) Arrangements of apparatus.	22
(4.2) The oscillator.	22
(4.3) Coupling.	24
(4.4) The detector.	25
(5) TESTING OF APPARATUS.	26
 ----- 	
References for Part I.	
 ----- 	
<u>PART II.</u>	
(6) THE TEMPERATURES OF A GAS DISCHARGE.	28
(7) METHODS OF MEASURING THE TEMPERATURES OF A GAS DISCHARGE.	32
(7.1) Introduction.	32
(7.2) Electron temperature.	32
(7.3) Gas temperatures from density measurements.	36
(7.4) Excitation temperature.	38
(7.5) Equilibrium temperature.	41
(7.6) Comparison of different methods with the same discharges.	43
(8) MEASUREMENT OF ATOMIC AND IONIC TEMPERATURES FROM THE DOPPLER BROADENING OF SPECTRUM LINES.	45
(8.1) Doppler broadening.	45
(8.2) Other causes of line broadening.	46
(9) REVIEW OF PREVIOUS MEASUREMENTS OF TEMPERATURE FROM THE DOPPLER BROADENING OF SPECTRUM LINES.	48
(10) THE CHOICE OF EXPERIMENTAL CONDITIONS	54
(10.1) Spectrum lines.	54
(10.2) Discharge pressure)	55
(10.3) Power Supply	56
(11) PRELIMINARY EXPERIMENTS WITH PULSED D.C. DISCHARGES.	58
(12) APPARATUS FOR EXPERIMENTS WITH R.F. DISCHARGES	59
(12.1) Arrangement of apparatus.	59
(12.2) The oscillator.	59
(12.3) The gas circulating system.	62
(12.4) Spectroscopic apparatus.	64
(12.5) Discharge tubes.	65

SUMMARY

	<u>Page.</u>
(13) INSTRUMENTAL EFFECTS.	
<u>PART I.</u> (13.1) Summary.	70
(13.2) The variation in the temperature of the spectrograph.	70
(13.3) The focus of the collimator.	73
(13.4) The width of the spectrograph slit.	73
(13.5) The width of the microphotometer slit.	75
(13.6) The grain of the photographic plate.	75
(13.7) The instrumental line contour.	76
(14) EXPERIMENTAL PROCEDURE.	77
<u>PART II.</u> (15) THE METHOD OF FINDING THE LINE CONTOURS.	80
(16) THE SPECTRA.	82
(16.1) Useful helium lines	82
(16.2) Effect of the constriction in the discharge tube.	82
(16.3) Impurities	83
(16.4) Use of lines of Hg. and Si as 'norms'.	85
(16.5) The line contours	86
(16.6) Spectra used for the estimation of temperature.	87
(16.7) Measurements of temperature drift made with the neon bulb spectrum	87
(16.8) Correction of line breadths for the effect of temperature drift	88
(16.9) Stark broadening of the helium lines.	90
(16.10) The intensities of the helium lines.	91
(17) RESULTS, AND DISCUSSION.	94
(17.1) Gas temperature, deduced from line breadths	94
(17.2) Excitation temperature.	96
(17.3) Equilibrium temperature.	98
(18) SUGGESTIONS FOR FUTURE WORK.	100

APPENDICES

REFERENCES FOR PART II.

besides this it is possible that some contribution to the He I spectrum may have come from the relatively cool afterglow. The relative intensities of

the lines gave an excitation temperature of the order of

1,500°K. for He I and 4000°K. for He II (lines at 2733 and

### PART I.

Besides the possible contribution of the afterglow to He I, the most likely reason for these low excitation temperatures is that the electrons' velocity distribution was not Maxwellian but contained a greater proportion of low energy electrons because of inelastic collisions with the

### PART II.

secondary electron emission from the walls of the constriction. An r.f. discharge in helium was examined with a quartz prism spectrograph in order to deduce the temperature of its excited atoms and ions from the Doppler breadth of their spectrum lines. A new 150 Mc/s. oscillator supplied a 20 micro-second pulse of about 25 K.W. into the discharge fifty times per second, and a constricted discharge tube was used in order to concentrate the power into a small volume of gas. The discharge was run at low pressure in order to reduce Stark broadening and was made part of a gas circulating system in order to avoid losses from 'clean-up'. The temperature drift of the spectrograph caused considerable difficulty, but the line breadths were corrected for this effect to a first approximation. At 0.03 mm. Hg. the breadth of the He I lines at 2723, 2764, 2829 A. corresponded to about 2,000°K. and that of the He II line at 2733 A. corresponded to 20,000°K.; this difference is attributed to Stark effect, but besides this it is possible that some contribution to the He I spectrum may have come from the relatively cool afterglow. The relative intensities of

the lines gave an excitation temperature of the order of  $1,500^{\circ}\text{K}$ . for He I and  $4000^{\circ}\text{K}$ . for He II (lines at 2733 and 3203 A.). Besides the possible contribution of the afterglow to He I, the most likely reason for these low excitation temperatures is that the electrons' velocity distribution was not Maxwellian but contained a greater proportion of low energy electrons because of inelastic collisions with the walls and secondary electron emission from the walls of the constriction. The relative intensity of the He I and He II spectra gave an equilibrium temperature of the order of  $16,000^{\circ}\text{K}$ .

THE IMPEDANCE OF AN R.F. DISCHARGE.



## (I) REVIEW OF PREVIOUS WORK

(1.1) The earliest studies in this subject were of the high-frequency properties of gas discharges maintained by d.c. fields. These and later studies of d.c. discharges are discussed in (1.2)(1.3). Recent work on the high-frequency properties of high-frequency discharges is discussed in (1.4) (1.5) (1.6).

(1.2) In early work with d.c. discharges the gas was made the dielectric of a condenser which was in parallel with a variable condenser in the tuned circuit of an oscillator. When the discharge was struck it altered both the dielectric constant and conductivity of the gas, which was equivalent to changing the capacity of the condenser and putting a resistive leak in parallel with it. It can be shown that for forced oscillations of a tuned circuit, the condition for maximum voltage across the condenser is independent of a high resistance in parallel with it. The method, therefore, was to adjust the tuned circuit for voltage resonance, then run the discharge and find what change in the capacity of the variable condenser was needed in order to obtain resonance again.

The difficulty with this method was that the formation of positive ion sheaths at the boundaries of the discharge tended to mask the effect that was sought. Such sheaths form at gas discharge boundaries because the electrons at first diffuse there much more rapidly than the positive ions and so leave behind them a positive ion space charge.

The walls of the tube, and any condenser plates in the discharge, charge up to a negative potential which reaches an equilibrium value (of a few volts) sufficient to draw in positive ions to them as fast as electrons can diffuse there against the potential gradient; this diffusion of electrons and positive ions at equal rates is known as ambipolar diffusion. Since all positive ions which diffuse to the plasma edge of the sheath are pulled to the boundaries, the positive ion current in the sheath is proportional to the positive ion density  $N$  in the plasma; and since the positive ion current is space-charge limited it is inversely proportional to the square of the sheath thickness, consequently the sheath thickness is inversely proportional to  $\sqrt{N}$ . At low ion currents the sheath can fill the whole volume between the r.f. condenser plates whose capacity then varies only as the dielectric constant of the ions varies, i.e. proportional to  $(1 - \text{const. } N)$ . At a critical value of  $N$  the sheath thickness on each plate becomes less than half the distance between them so the sheaths are equivalent to two condensers with positive ion dielectric which are joined in series by the conducting plasma (in which the concentrations of positive ions and electrons are equal). With further increase of  $N$  the apparent capacity at first increases with  $\sqrt{N}$  because the sheaths become thinner, but soon reaches a maximum and then decreases again because the dielectric constant decreases proportional to  $(1 - \text{const. } N)$ . (as expected from electromagnetic theory), but instead of decreasing uniformly with

discharge Appleton and Childs (1930) noticed such a variation of the apparent capacity with  $N$  and suggested the above explanation for it. They studied glow discharges in air at the order of  $10^{-2}$  mm. Hg pressure and currents up to 5 mA. They used condenser plates 2 cm. apart inside the discharge tube and a frequency of 100 Mcs. While the sheaths filled the gap the apparent dielectric constant decreased with discharge current, but once they failed to fill it the dielectric constant began to increase again, as described above.

dielectric Appleton and Chapman (1932) used condenser plates outside a 3 cm. diameter discharge tube and a frequency of 1000 Mcs. so that sheaths would not have time to form across the whole tube but would be confined near the walls. The discharges were in air at pressures from  $5 \times 10^{-2}$  to  $2 \times 10^{-1}$  mm. Hg. and at currents of up to 0.5 mA. They measured the r.f. current between the condenser plates (at voltage resonance) by means of a crystal rectifier and galvanometer and plotted its variation with pressure, keeping the electron concentration constant (found from Langmuir probe characteristics). The pressure at which this was a maximum agreed with the theoretical assumption that the damping force experienced by an electron in forced vibration in a sinusoidally varying field was equal to the product of its mass and collision frequency. The apparent dielectric constant of the ionised gas was always less than unity (as expected from electromagnetic theory), but instead of decreasing uniformly with

discharge current it still reached a minimum and then began to increase again. This minimum was attributed to the plasma electrons oscillating in resonance with the r.f. field, rather than to the sheath separating into two, because at no time could the sheath have filled the discharge tube. The position of the minimum agreed with the electron density expected for plasma resonance at that frequency on the basis of Tonk's and Langmuir's theory. Nevertheless it seems probable that the change in sheath thickness at the highest current densities could have had the effect of increasing the apparent dielectric constant.

Gangopadhyaya and Khastgir (1938) obtained a similar result except that the position of the minimum did not agree with plasma electron resonance. However, their experimental arrangement was very different from Appleton's in that their (external) condenser plates were parallel to and outside the (coaxial) d.c. electrodes, instead of being perpendicular to them. This was assumed to make wall-sheaths ineffective, but that is extremely unlikely and in fact the arrangement must have suffered from the more serious disadvantage that most of the potential drop between the condenser plates would be localized in the Crooke's Dark Space near the d.c. cathode. Their experiments were carried out in air and nitrogen discharges of up to 12 mA., using r.f. of 10 - 100 Mcs.

(1.3) A more recent method of studying the r.f. properties of a d.c. discharge has been to load a coaxial line

with it and to calculate its impedance, resistance and reactance from the standing wave ratio and the position of the first minimum on the line. Cobine, Cleary and Gray (1950) used this method to study arcs of up to 4 amps d.c. in air and inert gases at atmospheric pressure. They found that the impedance, resistance and reactance of the arc all increased with its length (which was never more than a tenth of the r.f. wavelength of 30 cms.) The r.f. resistance varied between 20 and 100 ohms and was of the same order as the d.c. resistance. It decreased as the arc current was increased; it increased as the arc length was increased but generally not linearly with it<sup>and</sup> for argon the curve of r.f. resistance versus length showed a definite maximum. The reactance was capacitative, between 20 and 60 ohms, it varied but little with the d.c. arc current; it increased non-linearly with the arc length and for helium and argon the curve of reactance versus length showed a definite maximum. The finding of a capacitative reactance agreed with the prediction in Everhart's and Brown's theory (1949) that a high conductivity discharge would have a capacitative reactance when the angular frequency of the r.f. was less than or equal to a quarter of the collision frequency of the electrons and the electron current was high; in these experiments the angular frequency of the r.f. had been about one eighth of the collision frequency of the electrons. There was no obvious explanation of the maxima.  $\sigma$ , conductance  $G$ , and susceptance  $B$  of the discharge, rather than their reciprocals (impedance,

(1.4) Everhart and Brown (1949) have developed the theory of the r.f. properties of high-frequency discharges, for which the following conditions are assumed:-

- (a) The dimensions of the discharge are much less than the wavelength of the exciting r.f. field.
- (b) The mean free path and amplitude of oscillation of the electrons are both much less than the dimensions of the discharge.
- (c) In the discharge the rate of ionization equals the rate of removal of electrons and ions from the discharge, and the dominant process for their removal is ambipolar diffusion (1.2).
- (d) The diameter of the discharge is much greater than its length, therefore radial diffusion may be neglected and the mathematical problem is one-dimensional.

(e) The volume rate of ionization is constant throughout the discharge. This neglects the second-order effect that the rate of ionization is a function of the r.f. field which is itself a function of position because the r.f. oscillating component of the space charge near the electrodes shields the central portion of the discharge.

(f) The discharge is in a region of parallel lines of electric field, therefore fringing fields and currents may be neglected.

In their mathematical analysis it is more convenient to consider the admittance  $Y$ , conductance  $G$ , and susceptance  $B$  of the discharge, rather than their reciprocals (impedance,

resistance, reactance). The admittance  $Y$  is the ratio of the total current in the discharge to the r.f. potential difference applied to the electrodes and it is complex because these two quantities are seldom in phase. The total current includes both the electron current and the displacement current  $dD/dt$ . (Before the discharge strikes, the electron current in the leads to the electrodes equals the displacement current between the electrodes; when the discharge is running, the electron current in the leads equals the sum of the electron and displacement currents between the electrodes).

The theory shows that when the electron current is much less than the displacement current the discharge impedance is equivalent to a parallel resistance and inductance whose magnitudes decrease proportionately as the electron current increases.

At electron currents comparable with the displacement current the discharge impedance is more complicated. Its resistance and reactance no longer decrease proportionately and its reactance may even become capacitive. For a capacitive reactance the ratio of electron current  $i$  to displacement current  $dD/dt$  must be sufficiently large, and the ratio of the angular frequency  $W$  of the r.f. to the electron collision frequency  $f$  must be sufficiently small. These conditions are expressed in terms of parameters  $n$  and  $g$  where  $n = (i)/(dD/dt)$  and  $g = w/f$

Everhart and Brown have solved the theoretical equations and plotted  $G$  and  $B$  as functions of  $n$  and  $g$ . It

appears that  $g$  is the more important parameter in controlling the sign of the reactance. At still greater electron current this theory does not apply because "skin effect" prevents condition (e) from being fulfilled.

It seems possible to give a simple physical picture of how the sign of the reactance should depend on  $g$ . When  $g$  is small then collisions will be frequent enough to keep the electrons in phase with the r.f. field, so the electron current will give a resistive component to the impedance: but the displacement current (which would be present even in a vacuum) will give a capacitive component. As  $g$  is increased the collisions will not be frequent enough to prevent the inertia of the electrons from carrying them out of phase with the r.f., so the electron current will lag behind the r.f. field and this inductive effect may be greater than the capacitive effect of the displacement current. Such a simple picture does not, however, show how the discharge could be inductive when  $n$  is small but capacitive when  $n$  is not too small, since it would be expected that the displacement-current effect should be dominant at small values of  $n$  and so make the reactance capacitive.

(1.5) R.f. discharges complying with the conditions assumed in the theory (1.4) have been studied experimentally by Brown and others at M.I.T. These discharges have occupied a cylindrical region, of dimensions much less than the wavelength of the r.f., between close parallel plates at the centre of a re-entrant resonant cavity, and have been maintained

by continuous power from a 3000 Mc/s. magnetron. Everhart and Brown carried out a series of experiments in which the magnetron was tuned to the resonant frequency of the cavity and maintained a helium discharge in the parallel plate region of the cavity. During each experiment the frequency and pressure were kept constant and the discharge current was varied by controlling the input power; this was equivalent to keeping  $g$  constant while varying  $n$ . The diameter of the discharge was measured with a travelling microscope. The experiment was repeated at different pressures, corresponding to different values of  $g$ . From these data,  $G$  and  $B$  were plotted as functions of  $n$  and  $g$ . These experimental curves agreed well with the theoretical ones (1.4). The gap between the parallel plates was 1 m.m., the diameter of the discharge was of the order of several m.m.,  $G$  was of the order of  $10^{-3}$  to  $10^{-2}$  mho and  $B$  varied between  $-10^{-3}$  and  $+2 \times 10^{-3}$  mho. The pressure range was from 3.5 to 252 mm. Hg. corresponding to a range of  $g$  from 2 to 0, and the range of  $n$  was from less than 0.25 to greater than 2. There is no mathematical difference between the h.f. admittance of h.f. and d.c. discharges except that the spatial electron distribution and the geometry are different. The authors suggested therefore, that the increased capacitance reported in earlier experiments with d.c. discharges (1.2) may have been caused by the reactance changing from inductive to capacitative as the electron current increased.

(1.6) Two other techniques for measuring the complex admittance of r.f. discharges in microwave cavities have been developed at M.I.T. Rose and Brown (1952) developed a standing-wave method. When the discharge was struck, the parallel reactance of the discharge altered the resonant frequency of the cavity, that is, the frequency at which the standing wave ratio was a minimum; the parallel resistance of the discharge altered the losses, and therefore altered the magnitude of the standing wave ratio at the resonant frequency. These changes enabled the discharge admittance to be calculated. Gould and Brown (1953) found the change in resonant frequency of the cavity by measuring the ratio of the power transmitted through it to the power incident on it, as a function of frequency. They chose variables such that the data could be plotted as a straight line whose slope enabled the discharge admittance to be calculated. Their technique was arranged to be a null method so that a smaller probing signal could be used with consequently less possibility of disturbing the plasma.

(2) BASIC DIFFERENCES BETWEEN D.C. AND R.F. DISCHARGES

In the author's experiments it was desirable to get as much power as possible into the discharge. There were two possible types of discharge which could have been used, d.c. arcs and r.f. discharges, and it was advantageous to use the latter in both parts of this study for reasons given below. (The particular advantages of the r.f. discharge which apply only to Part II of these studies are discussed in 10.3.).

An r.f. discharge is more efficient than a d.c. one because each of its electrons can ionize many atoms, and none are lost to the electrodes. It is more uniform for it has no cathode glow or positive column but is (to a first approximation) all plasma. Finally, it suffers less from sputtering because its ions do not have time to reach a high velocity and few of them reach the electrodes, and metal sputtering may be eliminated by using only external electrodes.

The operation of a d.c. arc depends on thermionic emission of electrons from the cathode spot, ionization of gas atoms by electron impact (by single impact at low current densities but also by successive impacts at high current densities), and return of sufficient ions to the cathode to keep the cathode spot at a sufficiently high temperature. In order to gain enough energy to ionize the gas atoms, those electrons emitted from the cathode must be accelerated through the cathode fall, and those produced by ionization of the gas must be accelerated through longer distances in the lower potential gradient of the positive column. The electrons

do not travel straight through the discharge with a steady acceleration, but each has its direction changed almost at random by elastic collisions with gas atoms and after each one it is either accelerated or decelerated depending on its direction relative to the electric field. The random velocity immediately after collision averages out over many collisions so although the electrons have a large random velocity their drift velocity in the direction of the electric field is small. The drift velocity of the electrons is built up until their gain of kinetic energy from the electric field equals their loss of energy by elastic and inelastic collisions and diffusion. Their gain of energy between collisions is a function of the electric field and the pressure. The drift velocity of the electrons is so much greater than that of the positive ions that they carry at least 95% of the drift current, and to a first approximation may be considered to carry all of it.

The d.c. discharge suffers from a power loss equal to the rate at which the drift current carries energy to the electrodes. This loss is avoided in r.f. discharges because the electrons and ions oscillate locally in the r.f. electric field rather than being accelerated by it to strike the electrodes. Also, as the pressure is decreased, and the mean free path of the electrons increased, the electrons have much less chance of ionizing in their single transit between the electrodes of a d.c. arc than in their the r.f. but long compared with both the mean free path of

continuing local oscillations in an r.f. discharge, so the d.c. arc mechanism fails first. The r.f. mechanism does not however suffer from a decrease in efficiency with decrease of pressure, as described later in this section.

In d.c. fields the paths of the electrons and their gain of energy from the field depend only on the electric field and the pressure. In r.f. fields, they depend also on the frequency of the field.

A 'low frequency' discharge is one in which the field frequency is very much smaller than the collision frequency, it differs little from a d.c. one. The drift current oscillates in phase with the field and a large fraction of the electrons and positive ions generated in each half cycle are lost in the same half cycle by being swept to the electrodes (or to the walls if the discharge is electrodeless). The only difference from a d.c. discharge is this change of polarity each half cycle. At a rather higher frequency although the electrons are still lost to the electrodes each half cycle, the positive ions do not have time to cross the tube in a half cycle and so are not lost. At a still higher frequency the electrons are not lost to the electrodes either, because there is not time for them to cross the tube in a half cycle; the mechanism is then that of an 'r.f. discharge'.

The type of r.f. discharge that is most used in the laboratory is made short compared with the wavelength of the r.f. but long compared with both the mean free path of electrons is by diffusion to the walls, resulting from

the electrons and their amplitude of oscillation. Its mechanism does not depend on internal electrodes, thermionic emission, or acceleration of electrons through long distances. Before the r.f. field is applied any free electron which happens to be in the discharge tube moves about colliding elastically with the gas atoms; it loses energy in some collisions, it gains it in others, but its kinetic energy of translation averaged over many collisions is equal to the mean kinetic energy of agitation of the atoms. When the r.f. field is applied each free electron gains energy from it. In its collisions with the gas atoms it sometimes loses energy, sometimes gains it; but on the whole it loses less to the atoms than it gains from the field so its kinetic energy increases over many half cycles of the r.f. It eventually reaches a dynamic equilibrium in which its mean rate of loss of energy to the atoms equals its rate of gain of energy from the r.f. field. In this condition it loses more energy in some collisions with atoms than it gains in others, but its mean energy remains at a constant value greater than their mean kinetic energy of agitation. So after many half cycles an electron may have sufficient energy to excite or ionize an atom, and then its process of obtaining energy from the r.f. field begins again. In the discharge there are, of course, many electrons (produced by ionization in inelastic collisions of electrons with atoms) and at any instant their mean kinetic energy as a group is higher than that of the gas atoms. The principal loss of electrons is by diffusion to the walls, resulting from

their large random motion; there is virtually no loss of current carriers to the electrodes. The efficiency of the energy transfer from the r.f. field to the electrons depends on the ratio of the collision frequency to the r.f. The efficiency is highest when this ratio is high, because then collisions keep the electrons in phase with the field. However, when this ratio is low collisions are not frequent enough to keep the electrons in phase with the field, the momentum of the electrons carries them on out of phase, so there is an out of phase component of drift current and less efficient transfer of energy from the field to the electrons. In the limit of a very low collision frequency (i.e. very low pressure) or a very high field frequency the electrons would oscillate in antiphase with the field and there would be no net transfer of energy.

The discharge was to terminate a slotted section of transmission line. Its impedance, resistance and reactance were to be calculated (using a circle diagram) from the standing wave ratio and the position of the first minimum on the line, its power was to be measured calorimetrically, and thus the r.f. voltage and current would be deduced. A pulsed, high-power oscillator was to be used to run discharges at more than 10 kw. pulse power. If the main experiment were successful it was to be extended to include the effect of a magnetic field on the discharge.

The differences between d.c. arcs and r.f. discharges in general have been considered in Chapter 2. In this chapter therefore the differences between the particular r.f. discharges used by Brown and others, and those used by the author, will be discussed. The main differences were in power and frequency.

The power input to these discharges was intended to be pulses of more than 10 kw., in contrast to the continuous wave discharges of a fraction of a watt which were used by Brown. The result of this would be a much larger value

(3) THE PROGRAMME OF RESEARCH.

Dr.K.W.Champion (1950-2) and Dr.N.L.Allen (1951-3) had studied the electrical properties of high power d.c. arcs, both in and out of a magnetic field. The former had considered following that work with a study of the properties of high-power r.f. discharges, and it was this problem which was taken over by the author.

The discharge was to terminate a slotted section of transmission line. Its impedance, resistance and reactance were to be calculated (using a circle diagram) from the standing wave ratio and the position of the first minimum on the line, its power was to be measured calorimetrically, and thus the r.f. voltage and current would be deduced. A pulsed, high-power oscillator was to be used to run discharges at more than 10 kW. pulse power. If the main experiment were successful it was to be extended to include the effect of a magnetic field on the discharge.

The differences between d.c. arcs and r.f. discharges in general have been considered in Chapter 2. In this chapter therefore the differences between the particular r.f. discharges used by Brown and others, and those used by the author, will be discussed. The main differences were in power and frequency.

The power input to these discharges was intended to be pulses of more than 10 kW., in contrast to the continuous wave discharges of a fraction of a watt which were used by Brown. The result of this would be a much larger value

of the electron current, and therefore of  $n$ , and the discharge impedance was expected to have a large resistive component in which to dissipate the power (since none could be dissipated in the reactive part).

The frequency of 300 Mcs was to be a tenth of that used by Brown and the consequences of that are as follows. The displacement current ( $dD/dt$ ) would be correspondingly lower and for this reason also  $n$  would be higher. Discharge dimensions of cm. (instead of only mm.) would be small compared with the wavelength; consequently the electron mean free path would be small compared with the dimensions until it became of the order of mm., at pressures of the order of 0.1 mm. Hg. The amplitude of electron oscillation would also be several mm., for assuming an electron temperature of  $100,000^\circ\text{K}$  an electron of average velocity moving at about  $2 \times 10^8$  cm./sec. (see Chapter 6, equation 1;  $\frac{1}{2} m v^2 = \frac{3}{2} kT$ ) would travel about 3 mm. in a half cycle of the r.f.

The electrode geometry could be either parallel plate or coaxial and both types could be designed to keep radial diffusion small; though if the coaxial type were used the lines of force would not be parallel so the mathematics of (1.4) would be made more complicated.

Champion and Allen found that a magnetic field increased the impedance of a d.c. arc and decreased its minimum running pressure owing to the increased paths of the electrons spiralling in the magnetic field. It was not expected to have so large an effect on a r.f. discharge

because in this the effective ionizing paths of the electrons (sum of oscillations) would always be long.

Dr. [Name] did the [Name] work on this problem. The [Name] [Name] [Name] the oscillator, but took over [Name] [Name] [Name] apparatus without [Name].

(A) A [Name] [Name] [Name] [Name] [Name] field of 22,700 [Name] [Name] [Name] [Name] [Name] had been stored in [Name] [Name] [Name] [Name] [Name] 25 kv. (Champion 1952).

(B) A [Name] [Name] [Name] [Name] [Name] three [Name] [Name] [Name] [Name] [Name] phase of the [Name] [Name] [Name] [Name] [Name] either singly or at a [Name] [Name] [Name] [Name] [Name]. The second and third [Name] [Name] [Name] [Name] [Name] to occur from [Name] [Name] [Name] [Name] [Name]. (Champion and Allen 1953).

(C) A [Name] [Name] [Name] [Name] [Name] would provide a [Name] [Name] [Name] [Name] [Name] 115 amp.

(D) A [Name] [Name] [Name] [Name] [Name] which could provide a [Name] [Name] [Name] [Name] [Name] 100 amp. It had a characteristic [Name] [Name] [Name] [Name] [Name].

(E) A [Name] [Name] [Name] [Name] [Name].

(4b) (4a) APPARATUS PROVIDED.

(4.1) Dr. Champion had already begun work on this problem. The author designed and built his own oscillator, but took over from Dr. Champion the following apparatus without modification.

(A) An air cored solenoid in which a pulsed sinusoidal field of 22,700 gauss peak was produced by energy which had been stored in 8 microfarad condensers charged to 25 kV. (Champion 1950).

(B) A trigger circuit which produced a group of three trigger pulses synchronised to occur at any desired phase of the mains cycle. The group could be produced either singly or at a repetition frequency of once per second. The second and third pulses could be varied independently to occur from 0 to 3.5 millisecc after the first one. (Champion and Allen 1952).

(C) A five section artificial line which could provide a 2.5 millisecc pulse of up to 2.5 kV. and 115 amp.

(D) A twenty-six section artificial line which could provide a 20 microsecond pulse of up to 7 kV. and 100 amp. It had a characteristic impedance of 60 ohms.

(E) A slotted section of coaxial line. discharge for 20 microsecond at a repetition frequency of once per second, to give an average power of the order of a watt which could be measured calorimetrically.

(4.2) The Oscillator.

The Oscillator was designed to give a pulsed output.

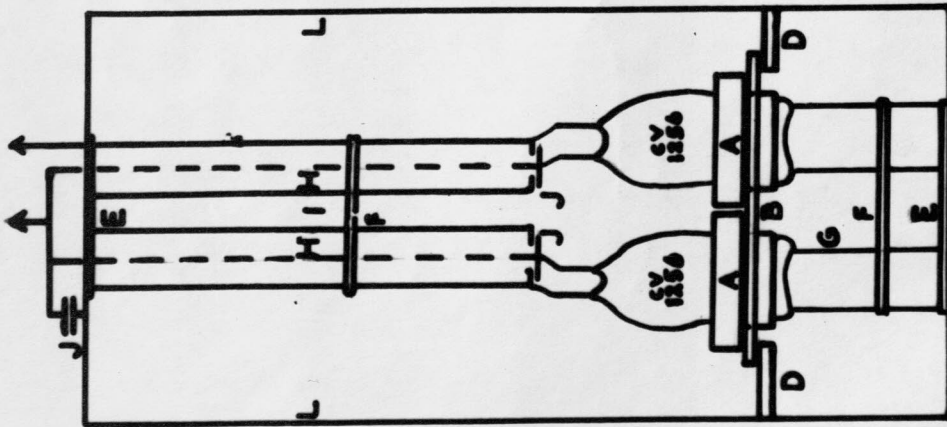
## (4b) DESIGN OF NEW APPARATUS.

### (4.1) Arrangement of Apparatus.

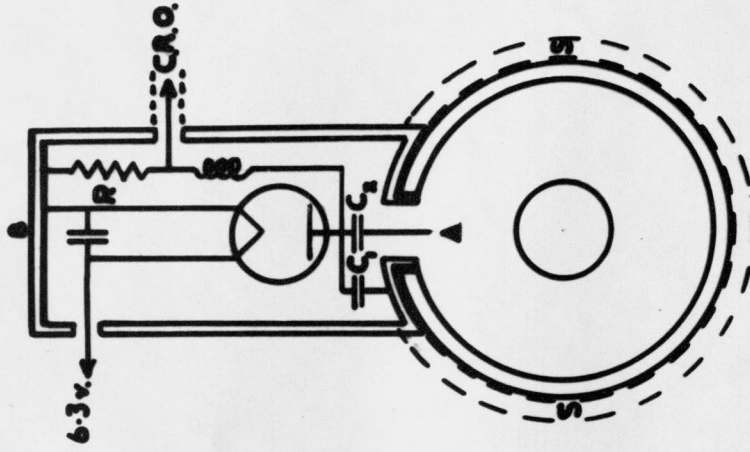
The slotted section of coaxial line, E, was to be terminated by a discharge tube which fitted into the end of it. The tube would have one electrode connected to the inner conductor of the line and the other one to the outer conductor; it would also have a subsidiary electrode. This part of the apparatus was to be small enough to fit inside solenoid A so that measurements of discharge impedance could be made either within or without a magnetic field. The trigger circuit, B, would control the sequence of events: firstly, a d.c. pulse from artificial line C applied to the subsidiary electrode would break down the gas and form a plasma in the tube; secondly, the magnetic field (if used) would begin its 10.7 m.sec. period; thirdly, as the d.c. pulse died away an oscillator would supply an r.f. pulse to the already ionised gas without losing r.f. power in having to break down the gas. The trigger circuit could vary the time interval between the first, second, and third events from 0 to 3.5 m.sec., and so the r.f. discharge could be made to occur at any value of the magnetic field up to its maximum. It was hoped to put about 50 kW. into the discharge for 20 microseconds at a repetition frequency of once per second, to give an average power of the order of a watt which could be measured calorimetrically.

### (4.2) The Oscillator.

The Oscillator was designed to give a pulsed output



1A. OSCILLATOR.



IB. DETECTOR.

of up to 50 kW. using the N.T. 99 (C.V.1256) triodes which were already in stock. A wavelength of about a metre was chosen because this was long compared with the dimensions of the discharge but not so long as to cause the standing-wave indicator to be unduly bulky. It was decided to use the two triodes in push-pull in a tuned-grid, tuned-cathode circuit with their anodes modulated by artificial line D. The great advantage of this circuit is that since there is only d.c. voltage between anode and earth and only r.f. voltage between cathode and earth, therefore, the voltage between any point and earth is kept to a minimum. A secondary advantage is that since there is no d.c. voltage on the cathode line it may be connected to the load either directly or indirectly. The N.T.99 is constructed with its anode forming part of its envelope. This makes N.T.99s very suitable for this circuit since two of them can be connected by a negligible anode-to-anode impedance by mounting them side by side with their anodes set in a common metal plate.

The construction of the oscillator is shown in diagram 1A. The valves were mounted side by side with their anodes protruding through close fitting holes in a small duralumin plate B. Their grids were connected by a parallel rod type of transmission line G of characteristic impedance 210 ohms, and made of copper. Their cathodes were connected by a similar line I of characteristic impedance 180 ohms. Both grid and cathode lines were short-circuited by a bar E

at their end remote from the valves and also carried another short-circuiting bar F which was variable in position. The grid line was used in the quarter wave mode: but the inductance of the cathode leads of the valve was so great that the cathode line had to be used in the three quarter wave mode. The filament leads H were screened from r.f. by passing them down the centres of the rods of the cathode line and were decoupled by condensers J. The whole oscillator was inside a metal screening box L to which was fixed the short-circuited end of both lines, and from which the anode mounting plate was well insulated by a distrene spacer D. Both anodes and grids were cooled by air blast. The oscillator's wavelength measured on a parallel line wavemeter was approximately 110 cm.

#### (4.3) Coupling.

Various forms of coupling to a dummy load were tried and the square of the voltage across the dummy load (measured with the detector described below) was assumed to be proportional to the output power. The dummy load was a carbon resistance of nominal value 10 ohms. At these high frequencies it would not have its nominal impedance but would probably act as a larger resistance in parallel with a small condenser (Blackburn 1948), therefore, the voltage across it could not be used to calculate the absolute power output of the oscillator but only to compare the effectiveness of various types of coupling. Various forms of indirect coupling were tried: condenser coupling, loop coupling,

and coupling with a loop which was in series with a condenser to give a series resonant circuit. However, it was found that direct coupling to the cathode line was most effective, therefore it was decided to use that between the oscillator and the slotted section of coaxial line.

(4.4) The Detector.

The detector part of the standing wave indicator was terminated by a dummy load. Various dummy loads, each made from a carbon resistance, were used. The top of the slotted screen of a cathode ray oscilloscope. All the circuit except probe A was inside a screening box B, and B was kept in good electrical contact with the slotted section by means of a spring S. This is shown in diagram 1B. Probe A was connected to the anode of a C.V.58 diode via a potential divider C<sub>1</sub> C<sub>2</sub>. The voltage drop across resistance R in the circuit was proportional to the current in the diode and therefore to the three-halves power of the voltage picked up by probe A. The oscilloscope had a sufficiently high input impedance for the envelope of the pulse (25 Kc/s Fourier fundamental component) to be able to follow it without gross distortion. The time constant of R and the capacity to earth (C<sub>1</sub> plus 20 pF input capacity of oscilloscope) was 0.9 microsecond, which was short compared with the pulse length (20 microseconds) but long compared with one period of the r.f (3 milli-microseconds), consequently the oscilloscope trace followed the pulse envelope but not the r.f.

on the harmonics.

It seemed then that these difficulties were caused

5. TESTING OF APPARATUS.

When the apparatus was tested it was found impossible to get consistent results; the reason for this failure was eventually traced to frequency instability of the oscillator. The cathode line of the oscillator was directly coupled to the slotted section of coaxial line and the line was terminated by a dummy load. Various dummy loads, each made from a carbon resistance, were used. The top of the slotted section and the sliding surface of the screening box of the detector were kept clean throughout the test to make good electrical contact. Attempts were made to match the line so that there would be no standing waves, and also to mismatch the line and check that the magnitude of the standing waves corresponded to the impedance of the load. Neither of these objectives could be attained. The standing wave frequency was found to be always a harmonic of the oscillator frequency (generally three times its frequency), the waves were often not sinusoidal, and it was difficult to get agreement between successive measurements. Mechanical measurements on the slotted section showed that there was no regular variation in its construction which could have caused apparent harmonics. It seemed possible that the harmonics might have been caused by the r.f. choke in the detector circuit resonating at that frequency with its own capacity; but changing to an entirely different r.f. choke had no effect on the harmonics.

It seemed then that these difficulties were caused

either by the load 'pulling' the oscillator frequency or by inherent frequency instability of the oscillator itself. There was no cathode ray oscilloscope to hand on which the oscillator frequency of 300 Mcs. could be observed; so it was decided to put an impedance matching device between the oscillator and the load so that the load could be certainly matched and not 'pull' the oscillator frequency. It was decided to use a parallel plate transmission line and stubs because of mechanical difficulties with coaxial stubs. The parallel plate line and stubs were made with the same characteristic impedance as the coaxial line, and the detector was modified for use with the parallel plate line. Both single and double stubs matching was tried, but without any success.

It was considered therefore that the difficulties were caused by frequency instability of the oscillator, and that the experiments could not be carried out unless a stable oscillator was built. The author had no experience of building stable r.f. oscillators, consequently, it was considered advisable for his work on this problem to be discontinued.

REFERENCES FOR PART I.

- Allen (1951) Thesis, University of Birmingham.  
(1951) Proc. Phys. Soc. (B). 64. 276.  
(1952) " 65. 697.  
(1953) " 66. 1087.
- Appleton and Childs (1930) Phil. Mag. 10. 969.  
Appleton and Chapman Proc. Phys. Soc. 44. 246.
- Blackburn (1948) 'Components Handbook' (McGraw Hill).
- Champion (1950) Proc. Phys. Soc. (B). 63. 795.  
(1951) Thesis, University of Birmingham.  
(1952) Proc. Phys. Soc. (B). 65. 329.
- Champion and Allen (1952) Electronic Engineering, 24. 423.
- Cobine, Cleary and Gray (1950) J.App. Phys. 21. 1264.
- Everhart and Brown (1949) Phys. Rev. 76. 839.
- Gangopadhyaya and Khastgir (1938) Phil. Mag. 25. 883.
- Gould and Brown (1953) J.App. Phys. 24. 1053.
- Rose and Brown (1952) J.App. Phys. 23. 711, 719, 1028.

THE TEMPERATURES OF A GAS DISCHARGE.

For molecules of a gas collide with each other so frequently that they are otherwise undisturbed they reach a dynamic equilibrium in which they have a Maxwellian distribution of kinetic energies of translation. The absolute temperature  $T$  is defined as a quantity which is proportional to the average kinetic energy of translation of the molecules at equilibrium. If  $v$  is their root-mean-square speed, the

PART II.

A SPECTROSCOPIC STUDY OF  
THE TEMPERATURE OF AN  
R. F. GAS DISCHARGE.

$\frac{1}{2}mv^2 = kT,$

This definition implies that the molecules are truly in equilibrium at a certain temperature of energies. In such cases as electrical discharges, though it may be in a steady state it is not necessarily Maxwellian.

Although the definition is not rigorously applicable to a discharge of a gas, the method of describing the average energy of the molecules, ions, electrons, in terms of an equivalent electron-volts; and although the discharge is unlikely to be Maxwellian, the temperature may by analogy be

(6) THE TEMPERATURES OF A GAS DISCHARGE.

The molecules of a gas collide with each other so frequently that if otherwise undisturbed they reach a dynamic equilibrium in which they have a Maxwellian distribution of their kinetic energies of translation. The absolute temperature  $T$  is defined as a quantity which is proportional to the average kinetic energy of translation of the molecules at equilibrium. If  $v$  is their most probable speed (the peak of the distribution curve)  $c$  their mean speed,  $s$  their root-mean-square speed,  $m$  their individual mass, and  $k$  is Boltzmann's constant, then the temperature  $T$  of the gas is defined by any of the following equations:

$$\frac{1}{2}mv^2 = kT, \quad \frac{1}{2}mc^2 = \frac{4}{\pi} kT, \quad \frac{1}{2}ms^2 = \frac{3}{2}kT \quad (6A)$$

This definition implies that the molecules are truly in equilibrium and have a Maxwellian distribution of energies. In such processes as diffusion, conduction and electrical discharges the gas is not in true equilibrium, though it may be in a steady state in which gain and loss of energy are equal, and its energy distribution may be approximately Maxwellian.

Although the concept of temperature is not rigorously applicable to a discharge it is a convenient way of describing the average energy of the particles (molecules, ions, electrons) instead of using ergs or equivalent electron-volts; and although the energy distribution is unlikely to be Maxwellian, the absolute temperature  $T$  may by analogy be

said to be related to the root-mean-square speed  $s_1$  of the given non-Maxwellian distribution by:

$$\frac{1}{2} m(s_1)^2 = \frac{3}{2} kT \quad (6B)$$

(Since the distribution is non-Maxwellian,  $s$ ,  $c$  and  $v$  are not related in the same way as in (6A).

In a self-sustaining gas discharge most of the gas is ionized and therefore conducting, with about 95% of the current being carried by the electrons. In the main ionized region, called the 'plasma', the concentrations of positive ions and electrons are both high and are approximately equal. Since the plasma is highly conducting and electrically neutral there is only a small average voltage gradient along it, but in other regions there may be much higher gradients e.g. in the Crooke's dark space of a glow discharge.

The electrons in a discharge gain much more energy from the electric field than do the ions, and neutral atoms of course gain none. So from this point of view the discharge may be regarded as a heated "electron gas" mixed with an unheated "heavy particle gas" with a continual transfer of energy from the former to the latter. This energy is transferred by elastic and inelastic collisions between electrons and heavy particles. Elastic collisions raise the temperature  $T_g$  of the heavy particles, inelastic collisions excite or ionize them instead, but both types of collision decrease the electron temperature  $T_e$ .

A statistical equilibrium is set up between the energy gained by the electrons from the field and that lost

by them in collisions with atoms and ions. If the collision frequency is  $f$  and the electric field  $E$  volt/cm. then an electron of drift speed  $u$  gains  $Eu/f$  electron volts between collisions. At high pressures practically all the collisions are elastic and in each one an electron of mass  $m$  loses about  $2mw/M$  of its excess energy  $w$  to a heavy particle of mass  $M$ .

$$\text{For equilibrium } Eu/f = 2mw/M \quad (6C)$$

If  $w$  falls by  $dw$  in time  $dt$ , and to  $w_t$  in time  $t$

$$dw = -(2mwf/M)dt \quad (6D)$$

$$w_t = w \cdot \exp(-2mft/M) \quad (6E)$$

So  $w$  falls to  $1/e$  of its value in the 'relaxation time'  $t_r$ , and to less than 1% in  $5t_r$ . If  $c$  is the mean velocity of the electrons and  $l$  their mean free path,

$$t_r = M/2mf = Ml/2mc \quad (6F)$$

Orders of magnitude for an arc in air at atmospheric pressure are:  $M = 30,000m$ ,  $l = 10^{-4}cm.$ ,  $c = 10^8 cm/sec.$ , so  $t_r$  is about  $10^{-8}sec.$ ; also  $E = 20$  volt/cm.,  $u = 10^5 cm/sec.$ ,  $f = 10^{12}/sec.$  so (from 6C)  $w = 0.03eV.$  and therefore  $T_e - T_g$  is of the order of  $250^\circ C$ . In practice,  $T_e$  and  $T_g$  are approximately equal.

At low pressures the electrons lose most of their energy by inelastic collisions, so these losses must be added to the right hand side of (6C). Since both  $u$  and  $l/f$  are inversely proportional to  $p$  (if other factors are unaltered), it follows that  $T_e$  can be much higher than  $T_g$  at low pressures.

In the plasma the energy distribution is likely

to be Maxwellian, or approximately so. However, it is unlikely to be so at its boundaries; for at the electrode boundaries there is the greatest drift velocity in the direction of the electric field, and there is a flow of energy across the other boundaries (to the walls at low pressure, and across the steep temperature gradient at the natural boundary at high pressure).

Since gas discharges are not systems in true equilibrium their temperatures are not thermodynamic parameters which are independent of the gas; but they are convenient parameters for describing its physical state. Consequently, although for a substance in true equilibrium it would not be necessary to know any of its physical properties before measuring its temperature, it is necessary to know some before measuring the temperature of a gas discharge (e.g. the molecular weight must be known before the gas temperature can be found by the Doppler breadth method). Furthermore, since each method of temperature measurement corresponds more or less sharply to one component of the discharge, the results obtained by different methods can only be compared when it is known precisely which temperature was measured by each.

#### (7.2) Electron Temperature.

The electron temperature may be found either from the current vs. voltage characteristics of a Langmuir probe or from the intensity distribution in the continuous reconstruction spectrum.

(a) In the first method a small probe is inserted in the

(7) METHODS OF MEASURING THE TEMPERATURES  
OF A GAS DISCHARGE.

(7.1) Introduction.

A comprehensive review of methods of measuring the various temperatures of a gas discharge has been given in a report by Edels (1950) to which the reader is referred for details and further references: shorter reviews are given by Suits (1941) and Mohler (1941). In this section brief notes are given on some of these methods and most attention is paid to those which have most connection with the author's work.

At high pressures all the components have the same temperature, which for a carbon arc in air at one atmosphere pressure is of the order of  $5000^{\circ}\text{K}$ . At low pressures the electron temperature is by far the highest being of the order of several tens of thousands of  $^{\circ}\text{K}$ ; the ionic, atomic and molecular temperatures tend to be the same because the ions gain about as much energy from the electric field as the neutral particles gain from collisions with electrons, and they may be as low as  $100^{\circ}\text{C}$  at low currents and pressures.

(7.2) Electron Temperature.

The electron temperature may be found either from the current vs. voltage characteristics of a Langmuir probe or from the intensity distribution in the continuous reconstruction spectrum.

(a) In the first method a small probe is inserted in the

discharge and the current  $I$  collected by it is measured as its potential  $V$  with respect to one of the discharge electrodes is varied.  $I$  is the sum of all electrons whose component of velocity perpendicular to the surface of the probe enables them to reach it against its retarding potential  $(V)_p$  with respect to the plasma, and which strike the probe each second. It can be shown that for a Maxwellian energy distribution:

$$I = \text{const.}_1 \exp. \left\{ -(V)_p \cdot e/k T_e \right\} \quad (7A)$$

where  $k$  is Boltzmann's constant and  $T_e$  is the electron temperature. Since  $(V)_p$  and  $V$  differ by a constant amount a plot of  $\log I$  against  $V$  gives a straight line from which  $T_e$  may be deduced; this is not valid for r.f. discharges since  $(V)_p - V$  is not then constant. When  $V = 0$  the probe is at "wall potential" and  $(V)_p$  is a few volts negative. It is separated from the plasma by a positive ion sheath of thickness  $d$  (see 1.2). The ion current to the probe equals the rate of flow of ions across the sheath boundary multiplied by the charge  $e$  of each; since it is space-charge limited it is proportional to  $(V)_p^{3/2}/d^2$ . Equating these two expressions:

$$(Nc/4)e = \text{const.}_2 (V)_p^{3/2} / d^2 \quad (7B)$$

where  $N$  is the positive ion concentration and  $c$  their mean speed. As  $V$  is made increasingly negative, so is  $(V)_p$ . therefore  $d$  increases. As  $V$  is made more positive and is increased through the plasma potential, so  $(V)_p$  is decreased through 0, the positive ion sheath disappears, and since the ion temperature is low the ion current rapidly stops

and a negative space-charge builds up. This causes a sharp break in the plot of  $\log I$  against  $V$ , which gives the plasma potential.

In using probes it is assumed that the plasma potential remains constant, which is not true for r.f. discharges as mentioned above. It is also assumed that the probe does not alter the region studied, and this is satisfied in a plasma, which is protected from the probe by the sheath and has a high ion concentration which is virtually unaffected by the small current to the probe; it would not be satisfied in regions of rapidly varying potential such as Crooke's Dark Space. It is further assumed that the electron energy distribution is not altered within the sheath by collisions with molecules. Near the plasma potential the sheath thickness is much smaller than the electron mean free path at low pressures. However, at pressures of the order of 1 cm. Hg the mean free path becomes of the order of the sheath thickness (it is about 0.03 cm. in air at 1 mm. Hg. pressure). The situation gets rapidly worse with increasing pressure because the mean free path is inversely proportional to the pressure, whereas for it can be seen from equations (7B) and (6A) that for a given  $N$  and  $(V)_p$  the sheath thickness  $d$  varies as  $C^{-\frac{1}{2}}$  and therefore as  $T_{(ion)}^{-\frac{1}{4}}$ , and it has already been mentioned in (7.1) that  $T_{(ion)}$  varies by a factor of only about 50 as the pressure varies by a factor of 1000 or more.

(b) The continuous spectrum of the afterglow of a

discharge is the result of electron to ion recombination. It extends from each series limit  $n_2$  to higher frequencies because before their capture the electrons had a continuous range of energies; the frequency  $n$  radiated on capture of an electron of velocity  $v$  is given by:

$$hn = hn_2 + mv^2/2 \text{ where } h \text{ is Planck's constant.}$$

The intensity of the continuous spectrum at frequency  $n$  depends on:

- (a) the variation with velocity of the cross-section for radiative capture, and of the cross section for the reverse process in which the photon  $hn$  is absorbed by an atom;
- (b) the product of the positive-ion and electron concentrations;
- (c) the velocity distribution of the electrons (usually Maxwellian).

The experiments of Mohler (1933-37) with low pressure Cs- vapour discharges verified the Quantum theory prediction that the cross section depended on  $1/v$  for hydrogen-like atoms. So using the theoretical expression for (a) he deduced (b) and the electron temperature from measurements of the relative intensity of the recombination spectrum at two wavelengths.

Cillie (1936) deduced the variation with electron temperature in the intensities of the lines of the Balmer series relative to the intensity at the head of the Balmer continuum. There was agreement between the theoretical and observed values for the solar chromosphere, but not for

certain planetary nebulae. Ravenhill and Craggs (1951) used a similar method to find the electron temperature in the afterglow of discharges in hydrogen at one atmosphere pressure.

(b) Under certain conditions the electron temperature is equal to the "excitation temperature" which is deduced from the relative intensities of lines in a spectral series. This is mentioned in (7.4).

### (7.3) Gas temperature from density measurements.

The gas temperature of a discharge in an ideal gas could be found simply from the gas density. More data is generally needed for a real gas, e.g. for air the partial pressure and constitution of each of the dissociation products must be known over the measured range of temperature. There are several methods of measuring the density of a discharge.

- (a) A method using X-ray or alpha particle absorption was developed by von Engel and Steenbeck (1931-3), and Ramsauer did similar work using electron beams. The absorption in the cool gas at the boundary was very large, so absorption measurements were made with different lengths of discharge and the end effect was eliminated as a difference. They measured the temperature of arcs in air with an accuracy of  $\pm 350^\circ\text{K}$  for temperatures of about  $5000^\circ\text{K}$ . The use of alpha particles seems preferable, because they are not absorbed exponentially like X-rays and do not suffer such large fluctuations in range as do electrons, therefore the measurements should be less affected by the cool
- (c) A more sensitive method of measuring the change in gas density is to use a refractometer. This has been done by Milatz, Vreedenburg and Braak for a low-pressure neon discharge. The light beam was narrow enough to be used to probe different parts of the discharge and so obtain the radial temperature distribution, and temperatures as low as  $350^\circ\text{K}$  were measured to  $\pm 2\%$ .

boundaries. The method would be less accurate at lower temperatures because of smaller difference between the absorption with and without the gas discharge.

(b) Another method was developed by Suits in 1935, to (7.4) measure the velocity of a sound pulse through the discharge. Since the velocity depends on the ratio of the specific heats and the molecular weight, it is necessary to know these quantities for all the dissociation products of the gas in the temperature range which is studied. In Suits' experiments the sound pulse was generated by a spark in the hot gas of the discharge, so no end-correction was needed at the source. However, since the detector had to be outside the discharge the measurements were more accurate for long arcs than for short ones. The best detector was a second spark whose voltage (displayed on a c.r.o.) showed a sudden rise when the sound pulse reached it. Temperatures of the order of  $5000^{\circ}\text{K}$  were measured to  $\pm 200^{\circ}\text{K}$ ; the measurements would be less accurate at lower temperatures.

(c) A more sensitive method of measuring the change in gas density is to use a refractometer. This has been done by Milatz, Vreedenburg and Braak for a low-pressure xenon discharge. The light beam was narrow enough to be used to probe different parts of the discharge and so obtain the radial temperature distribution, and temperatures as low as  $330^{\circ}\text{K}$  were measured to  $\pm 2\%$ .

The method needs a probing beam which is much brighter than the discharge; the advantage of its high sensitivity could only be used to the full for steady discharges.

#### (7.4) Excitation temperature.

Spectroscopic methods have the advantage of causing the least disturbance of the discharge and of needing the minimum length of gas path. The majority of them are used to determine the excitation temperature  $T_x$ , which is the temperature corresponding to the distribution of excited atoms among the various excited states.

(a) The relative intensities of lines ending in a common energy state depends on their relative transition probabilities and the concentration of atoms in each excited state. The latter depends in turn on the balance between those processes forming the excited state and those degrading it. The formative processes include upward transitions from lower states and downward transitions from higher states. The degrading processes include transitions to higher or lower states. Upward transitions may be caused either by collision or by light absorption, downward transitions may be radiative ones or be "collisions of the second kind" in which the potential energy of the excited state is changed into kinetic energy of the separating particles. Further complications are caused by ionization, recombination, diffusion and three-body collisions. Since there is such a multiplicity of processes the practical success of this method of temperature

measurement depends on obtaining a discharge for which suitable simplifying assumptions can be made.

If excitation takes place mainly by collision with electrons and if the lifetime of the excited state is short compared with the average time between collisions of excited with unexcited atoms, then  $T_x$  corresponds to  $T_e$ ; this would be expected at low pressures and high current densities. If it takes place mainly by atomic collisions, or if there are many collisions of excited with unexcited atoms in the lifetime of the excited state, then  $T_x$  corresponds to  $T_g$ ; this would be expected at high pressures.

However, unless there is a known equilibrium distribution of the atoms in the excited states, the calculated value of  $T_x$  will not be constant throughout the spectral series. The wider the spacing of the energy states, the higher is the necessary energy input to the discharge before there can be an equilibrium distribution among them all. Consequently a monatomic gas with close energy levels would reach this equilibrium at a lower temperature than would one with widely spaced levels. Similarly, with increasing temperature in a molecular gas this equilibrium would be reached first among the rotational levels, secondly among the vibrational levels and finally among the electronic levels. At the high temperatures of the atmospheric carbon arc both rotational and vibrational energies would be expected to have reached it and the most successful measurements of  $T_x$  seem to have been made with CN,  $C_2$ , CH, AlO and other bands excited in such arcs. In other measurements there

have generally been discrepancies between values of  $T_x$  calculated from different spectral series excited in the same discharge, or even from different pairs of lines in the same series. A full review of experimental results has been given by Edels (1950).

(b) Excitation temperatures have also been found by two methods in which light from a black body is passed through the discharge. In the method of anomalous dispersion, the continuous black body spectrum is passed through a Jamin refractometer of which one limb contains the discharge and the other is evacuated; the fringes are then passed through a spectrograph, giving both a continuous spectrum and the discharge spectrum crossed by interference fringes. In the method of anomalous dispersion near the absorption lines of the gas the fringes are bent corresponding to the rapid change in refractive index. From measurements of the relative intensity of spectrum lines with the same upper level, and of the fringes in their neighbourhood, it is possible to deduce the relative concentrations of excited atoms in the various energy levels. In the second method the light from the black body is projected through the discharge onto the slit of a spectrograph. The line spectrum of the discharge appears superimposed on the continuous spectrum and lines which are strongly absorbed may appear either dark or bright, depending on the temperature of the black body. The temperature of the black body is altered until the background matches the line; this is called the 'reversal temperature' and has been shown

analysis of Stark broadening for each important component to be the same as the excitation temperature. The method is limited by the fact that most discharges operate at reversal temperatures higher than those of available black bodies.

#### (7.5) Equilibrium temperature.

The Saha equation for a thermal ionization reaction can be applied only if the components are in equilibrium so it may be used for high pressure discharges but not for low pressure ones. The concentrations of the various components must be known, and for a monatomic gas these may be deduced from the pressure, voltage gradient, and current density. A typical use of this method was by Elenbaas, who checked it against the sound velocity method for a mercury discharge at 1 atmosphere pressure and then used it at 200 atmospheres where the other method could not be used. The temperature of the mercury arc at 200 atmospheres was found to be  $8900 \pm 800^\circ\text{K}$ .

The Saha equation has also been used to deduce the temperatures of spark channels in hydrogen, by Craggs and Meek (1946) and by Craggs and Hopwood (1947). The percentage ionization in the channel was found from the Stark broadening of the Balmer lines, and this was then substituted in the Saha equation to give the temperature. The line contours were found in two ways: by photographing the spectrum and plotting the line contour with a microphotometer; and by plotting them directly with a photo-multiplier, amplifier, and cathode-ray oscilloscope; the methods gave identical contours. Theoretical contours deduced from Holtsmark's

analysis of Stark broadening for each important component of H-alpha, H-beta, H-gamma, were added to give resultant theoretical contours for various average intermolecular fields; the Holtzmark analysis applies only to the wings of the lines. The average intermolecular field was found by comparing the wings of the lines with the theoretical contours, then the ion concentration was calculated from Holtzmark's equations. The percentage ionization was calculated from the ion concentration and the pressure, and this was substituted in Saha's equation to find the temperature. The value obtained by this method (described fully in the 1947 paper) agreed with that deduced from the pressure, voltage gradient, and current density (1946). The ion concentration was about  $2.5 \times 10^{17}/\text{cc}$  and the temperature about  $12,000^\circ \text{K}$ . It was considered that thermal equilibrium would be virtually established in the spark channel during even the shortest pulses used (1 microsecond) because during that time many thousands of electronic collisions would have occurred.

The main practical differences between the use of line contours in this method and their use in the Doppler-breadth method described in chapter 8 are as follows. This method is applicable only at high pressures (because there must be equilibrium) and Stark broadening is used; the other method can be used only at low pressure because at higher pressures Stark broadening is a nuisance. At  $12000^\circ \text{K}$  in the spark this method gives lines  $25 - 130 \text{ cm}^{-1}$  half breadth; at about the same temperature the Doppler

broadening gives only about  $2 \text{ cm}^{-1}$  half breadth so needs to be studied with apparatus of much higher resolving power. This method uses the shape of the wings of the lines; the Doppler method uses the half-intensity breadth of the line.

(7.6) Comparison of different methods with the same discharge.

There are comparatively few experiments in which the temperature of the same discharge has been measured by several different methods. Kruithof (1943, 1944) found agreement between excitation and equilibrium temperatures for a carbon arc (with Ca and Sr impurities introduced) in air, but this result is not conclusive because the calculation was carried out in part on the assumption that Saha's equation was valid for the discharge. Edels and Craggs (1951) have measured the electron, excitation, and equilibrium temperatures of hydrogen arcs at 1 to 2 atmospheres pressure. The electron concentration  $N$  was deduced from the Stark broadening of the Balmer lines, this was substituted in the drift current equation ( $I = Nev$ ) and the drift velocity  $v$  so deduced corresponded to an electron temperature of about  $5000^\circ\text{K}$ . The excitation temperature was found to be of the same order of magnitude as  $T_e$  on comparing H-beta and H-gamma, but about twice as great on comparing H-alpha and H-gamma. The equilibrium temperature was found by the method described in (7.5) to be about  $9000^\circ\text{K}$ . Such discrepancies between equilibrium and excitation temperatures have also been found for H and He in the solar chromosphere.

Maecker (1953) has successfully used several

spectroscopic methods together in order to measure the temperature distribution in a 200 amp. carbon arc at atmospheric pressure. The relative electron concentrations in different regions were first deduced from the intensity distribution in the continuum (7.2.b), then the absolute electron concentration in the core was deduced from the Stark breadth of the H-beta line (7.5). The equilibrium temperature in the core was found from relative intensity of lines of an element in its ionized and neutral states (17.3 and Appendix 3) and Saha's equation. There was agreement between equilibrium temperatures found from CI and CII lines, from Cd I and Cd II lines, and the excitation temperatures of OI lines; these were nearly  $11,000^{\circ}\text{K}$  at the axis. Lines of ionized atoms were not appreciably excited in regions at less than  $10,000^{\circ}\text{K}$ ; but the excitation temperatures of these regions could still be found from the lines of neutral atoms, using Hg and C lines (which agreed) over the range 9000 to  $6000^{\circ}\text{K}$ ., and the Na-D lines in the  $4000^{\circ}\text{K}$  range.

Comparisons of the Doppler-breadth method (Chapter 8) with other methods are described in (9.4, 9.7).

The following deductions may be made from these equations.

(a) The line breadth is directly proportional to the wavelength of the line. Consequently, if a grating spectrograph is used it is best to study a line at the red end of the spectrum; however, if a prism spectrograph

(8) MEASUREMENT OF ATOMIC AND IONIC TEMPERATURES FROM  
THE DOPPLER BROADENING OF SPECTRUM LINES.

(8.1) Doppler broadening.

The contour of a spectrum line which has been broadened by Doppler effect has the same shape as the distribution curve for the line-of-sight velocities of the emitting atoms and ions of the gas discharge and so is approximately the shape of the 'Gaussian Error Curve'. Therefore at a distance  $x$  from the centre of the contour the intensity is

$$I = \text{const.} \exp(-x^2/2)$$

and a plot of  $\log I$  to  $x^2$  gives a straight line. The difference between the two values of  $x$  at which  $I$  has fallen to half its maximum value is called the 'half-intensity breadth' or 'line breadth',  $b$ . It can be shown (White, 1934) that

$$b = 1.67 (n/c) (2 RT/M)^{\frac{1}{2}} \text{ in cm.}^{-1} \quad (8A)$$

$$b = 1.67 (l/c) (2 RT/M)^{\frac{1}{2}} \text{ in cm.} \quad (8B)$$

where:  $n$  is the wavenumber of the line and  $l$  is its wavelength,  $c$  is the velocity of light,  $R$  is the gas constant,  $M$  is the molecular weight of the gas,  $T$  is the temperature in  $^{\circ}\text{K}$ .

The following deductions may be made from these equations.

(a) The line breadth is directly proportional to the wavelength of the line. Consequently, if a grating at high spectrograph is used it is best to study a line at the red end of the spectrum; however, if a prism spectrograph

is used the breadth of the line seen on the photographic plate will probably be dominated by the abnormal dispersion of the prism and it is then best to study a line at the violet end of the spectrum.

(b) The line breadth is inversely proportional to the square root of the molecular weight of the gas therefore it is best to use either a hydrogen or a helium discharge.

(c) The line breadth is proportional to the square root of the absolute temperature, consequently this method of temperature measurement is not very sensitive or accurate.

(d) The Doppler broadening is independent of the pressure. Line broadening from other causes generally increases with the pressure, therefore measurements of Doppler breadth are best made at low pressures.

#### (8.2) Other causes of line broadening.

The natural breadth of a spectrum line is only of the order of a ten-thousandth of an A. and was therefore negligible for this experiment. Although pressure and resonance broadening would be of the order of the Doppler breadth at N.T.P., they are both proportional to pressure and so would be negligible at the pressures used in the experiments (1 mm. Hg to 0.02 mm. Hg). Distortion of the line contours by self-absorption was avoided by not using resonance lines, or other easily excited ones, and using short discharge tubes. The discharge had to be run at high current densities in order to obtain high gas temperatures, so Stark broadening was inevitable. However, since Stark

broadening is proportional to the pressure it was expected to be less than the Doppler broadening at the low pressures used. Fabry and Buisson (1912) showed that under suitable conditions the line breadth would also be affected by instrumental limitations. These limitations were studied experimentally and are described in chapter 13. Since there are so many possible causes of broadening and it is difficult to ensure that all the unwanted ones are negligible, the gas temperature deduced from the Doppler breadth must be considered to represent a maximum value for the temperature of the atoms. If the breadths of the helium line at 5876A., the neon line at 5852A, and the krypton line at 5570A, were caused only by Doppler broadening, then observed the value of  $N$  for each of the lines. At room temperature the agreement between the observed and calculated values of  $N$  was better than  $\pm 1\%$ ; at liquid air temperature the agreement was not so good, which they attributed to the discharge being above the temperature of the liquid air. However, the results agreed fairly well with the assumption that the breadth was proportional to  $(T/M)^{1/2}$ .

(9.2) Babcock (1923), at Mount Wilson, made measurements of the breadth, intensity and wavelength of the auroral green line at 5577A. with Fabry-Perot etalons. The source was the faint persistent light of the night sky, and since 5577A. is the only emission line within a long range of that spectrum the interference rings from the etalon were

(9) REVIEW OF PREVIOUS MEASUREMENTS OF TEMPERATURE FROM  
THE DOPPLER BROADENING OF SPECTRUM LINES.

(9.1) Fabry and Buisson (1912) showed that under suitable conditions of excitation the line breadth is caused simply by Doppler broadening. They used A.C. discharges in Geissler tubes filled with helium, neon, and krypton respectively, all at 1 mm. Hg pressure. They found the limiting order  $N$  up to which interference could be observed and assumed that the breadth of a line of wavelength  $\lambda$  was equal to  $\lambda/N$ . They calculated the value of  $N$  to be expected at room temperature and at liquid-air temperature if the breadths of the helium line at 5876A., the neon line at 5852A, and the krypton line at 5570A, were caused only by Doppler broadening, then observed the value of  $N$  for each of the lines. At room temperature the agreement between the observed and calculated values of  $N$  was better than  $\pm 1\%$ ; at liquid air temperature the agreement was not so good, which they attributed to the discharge being above the temperature of the liquid air. However, the results agreed fairly well with the assumption that the breadth was proportional to  $(T/M)^{-\frac{1}{2}}$ .

(9.2) Babcock (1923), at Mount Wilson, made measurements of the breadth, intensity and wavelength of the auroral green line at 5577A. with Fabry-Perot etalons. The source was the faint persistent light of the night sky, and since 5577A. is the only emission line within a long range of that spectrum the interference rings from the etalon were

photographed directly, (i.e. without crossing the etalon with a spectrograph). The highest order of interference used was 85,000 waves, obtained with a gilded plane parallel glass plate. A conservative estimate of the width of the auroral green line was that it did not exceed 0.035 Å. In 1923 the temperature of the atmosphere at that height (200-300 Km) was thought to be 500°K and therefore the then-unidentified auroral green line must have been emitted by an element at least as heavy as helium. It is now known that the auroral green line is produced by a 'forbidden transition' in oxygen atoms, consequently Babcock's results show that the temperature of the emitting atom is of the order of 1200°K, or less; other evidence now seems to indicate a temperature of the order of 1000°K (Mitra 1947).

(9.3) Orstein and van Wyk (1932) studied the line contour at 5016 Å. emitted from a hot cathode discharge in helium at  $2 \times 10^{-2}$  mm.Hg. pressure. The discharge was confined between coaxial cylinders of which the outer was kept at 650°K and the inner at 370°K. Observations were made perpendicular to the walls with a Fabry-Perot etalon crossed with a prism spectrograph. The line contour was corrected for instrumental broadening by using the theoretical results of Burger and van Cittert. The violet side of the contour corresponded to atoms leaving the cooler wall and travelling towards the observer; the red side corresponded to atoms receding from the hot wall, and

from the observer. The form of the distribution function was tested by plotting the logarithm of the intensity against the square of the distance from the centre of the line, which would give a straight line for a Maxwellian distribution. The violet side had an exactly Maxwellian distribution corresponding to  $400^{\circ}\text{K}$ ; the red side was Maxwellian except for a deviation near the centre of the line, and corresponded to  $480^{\circ}\text{K}$ . The difference between the temperature of the gas and the cold wall was explained by the heating of the gas by the discharge. That at the hot wall was explained by the incomplete exchange of energy between the wall and the gas molecules, giving an 'accommodation coefficient' for helium on glass of  $(480-400)/(650-400)$  i.e. of 0.32. When the heating coil for the outer cylinder was switched off the line contour became symmetrical, Maxwellian, and corresponded to  $320^{\circ}\text{K}$  for both walls.

(9.4) Gaydon and Wolfhard (1940) used the Doppler breadth of spectral lines to measure the translational temperatures of CH radicals in oxy-acetylene flames. In observations of the CH bands around 4315 and 3900 Å were made with a Fabry-Perot etalon crossed with a prism spectrograph. The instrumental contour was found from the spectrum of a watercooled Hg arc, for which Doppler and pressure broadening were small. The arc was much brighter than the flame, so several short exposures of it were made at intervals during the exposure to the flame spectrum; this gave mercury lines superimposed on the CH spectrum and

falling between the CH lines. The instrumental contour deduced from these mercury lines was integrated graphically with an ideal Doppler contour for an assumed temperature, and compared with the contours of the CH lines. At one atmosphere pressure it was found that there was very little pressure broadening of the CH lines and the translational temperature of the CH radicals was of the order of  $2600^{\circ}\text{K}$ , rather less than the theoretical maximum flame temperature. For pressures of 2 to 14 mm.Hg. the translational temperatures were of the order of  $4000^{\circ}\text{K}$ , much higher than the theoretical maximum reaction temperatures of  $2500 - 2800^{\circ}\text{K}$ . Temperatures deduced from the intensity distribution in rotational bands were of the order of the theoretical maximum ones. It was suggested that this showed that there was not normal thermal excitation of CH, but excitation by collision with other active species within the flame.

(9.5) Meinel (1950) and Gartlein (1951) have used grating spectrographs to deduce proton speeds in aurorae from the contour of the H-alpha line of auroral arcs. In the spectrum of a major auroral storm in August 1950 Meinel found that H-alpha viewed towards the magnetic zenith was very asymmetrical with the entire line shifted to violet; while viewed towards the magnetic horizon it was symmetrical, though broadened. The breadth corresponded to a velocity spread of 0 to  $3300 \text{ Km/sec}$ . This could not be the velocity

spread of the incident protons since it is known that all

arrive nearly simultaneously in the upper atmosphere, so it was suggested that this must be the result of their loss of energy by collision there. The violet wing of the line showed that they must have entered the atmosphere with a speed of at least 3300 Km./sec.; this is a lower limit because the proton has but small probability of emitting H-alpha through electron capture at higher speeds.

Gartlein and his collaborators in September 1950 observed the same part of the same arc of a moderate aurora with equal spectrographs at stations 300 Km. and 70° to 90° apart.

Previous spectra taken perpendicular to auroral rays had shown only broadening: but these, observed along the rays, showed a violet shift as well. This demonstrated that the particles emitting H-alpha were influenced by the earth's magnetic field and must therefore be protons. It was suggested that the breadth of H-alpha indicated either the velocity spread caused by scattering, or the line of sight components of the velocity of the protons spiralling down in the earth's magnetic field. The violet wing was displaced 10 A. in one photograph and 30 A. in the other, corresponding to line of sight velocities of 450 Km./sec. and 1350 Km./sec. respectively at the two stations.

(9.6) Foster (1953) deduced the energy of the He atoms and ions, in a high vacuum ion-pump which he was developing from the breadths of the He I line at 4438A. and the He II line at 4686 A., and found them to correspond to 3,200°K. and 5,200° respectively. He used a Fabry-Perot interferometer

crossed with a prism spectrograph.

(9.7) Schoen and Holmes (1954) compared temperatures deduced from  $N_2^+$  rotation bands with those deduced from the Doppler breadth of He lines in d.c. discharges through mixtures of  $N_2$  and He at unstated pressures. For the line breadth measurements the spectrograph was crossed with a Fabry-Perot interferometer. The He line contours were asymmetrical (probably owing to pressure broadening) and even their narrow half indicated at temperature of from 250 to  $400^\circ K$  as against  $108^\circ K$ . deduced from the band spectra..

(9.8) During the total eclipse of the sun on June 30th, 1954, Redman (1954) photographed the spectrum of the chromosphere using a plane grating of high dispersion, in order to measure its temperature. At the same time von Klueber and Jarrett photographed the coronal green line (5303A.) through a Fabry-Perot etalon in order to deduce the temperature of the corona.

TABLE I. Hydrogen Lines.

<u>Wavelength in A.</u>	<u>Breadth at 10<sup>4</sup> °K. in A</u>	<u>Dispersion mm/A</u>	<u>Breadth on plate mm x 10<sup>2</sup></u>
3970	28.6	0.09	2.55
3750	27.0	0.105	2.85
3691	26.6	0.11	2.9

TABLE 2. Helium Lines.

<u>Spectrum</u>	<u>Wavelength in A.</u>	<u>Breadth at 10<sup>4</sup> °K. in A.</u>	<u>Dispersion mm/A.</u>	<u>Breadth on plate mm x 10<sup>2</sup></u>
He I	2829	10.2	0.25	2.55
	2764	9.95	0.255	2.65
	2723	9.8	0.28	2.75
He II	2733	9.85	0.275	2.7
	2511	9.0	0.375	3.4
	2385	8.6	0.435	3.7
	2306	8.3	0.495	4.1
	2252	8.1	0.58	4.7

(10). THE CHOICE OF EXPERIMENTAL CONDITIONS.

(10.1) Spectrum lines.

The discharge spectrum was obtained by using a Hilger large quartz prism spectrograph which when used with the best slit width for the wavelength range studied (2000 - 4000 A.) formed lines with a minimum instrumental breadth of 0.025 m.m. It was calculated that this instrumental breadth was less than the Doppler breadth at  $10^4$  °K. for hydrogen lines of wavelength less than 4000 A. and for helium lines of less than 2900 A. This is shown for typical lines in tables 1 and 2, from which it is apparent that it is advantageous to study the helium lines; for although they are not so intense as the hydrogen lines are and are in a spectral region where the photographic emulsion is less sensitive, yet that is the region where the spectrograph produces the greatest dispersion. The He I lines are the highest members of a series of very close triplets (unresolved by any spectrograph, except for the lowest members of the series) of which one component is so much more intense than the others that they appear to be singlets: the He II lines are singlets. Stark broadening would be greater for the He II lines of the hydrogen-like helium ion than for the He I lines of the neutral helium atom. The discharge conditions were aimed to excite the He II line at 2511 A. sufficiently for its Doppler breadth to be measured.

TABLE 3.

Percentage ionization of helium at various temperatures and pressures

Temperature °K	Pressure in atmospheres				
	<u>1</u>	<u>10<sup>-1</sup></u>	<u>10<sup>-2</sup></u>	<u>10<sup>-3</sup></u>	<u>10<sup>-4</sup></u>
10,000	0	0	0	2	6
12,000	0	0	3	10	20
14,000	0	5	18	13	66
16,000	5	24	45	75	97

(10.2) Discharge Pressure.

A low pressure discharge was used for three reasons: to reduce unwanted causes of line broadening, to enhance the He II lines, and to reduce the heat capacity of the gas.

The effect of pressure on unwanted causes of line broadening has been discussed in (8.2). Its effect on the percentage ionization of helium is shown in table 3, in which it is assumed that equilibrium has been reached (Saha, 1950).

By reducing the pressure of a small volume of gas, and therefore its heat capacity, it was energetically possible for it to be heated by  $10,000^{\circ}\text{K}$ . with the r.f. oscillator which was available (12.2). The energy would be used in raising the atoms by  $10,000^{\circ}\text{K}$ ., raising the electrons to a much higher temperature of perhaps even  $100,000^{\circ}\text{K}$ ., and in ionizing the atoms.

To raise an atom by  $10,000^{\circ}\text{K}$ . would need  $(10,000/7,730)$   
= 1.3 eV.

" " " electron  $100,000^{\circ}\text{K}$ . " " 13 eV.

To ionize an atom would need 24.5 eV.

To excite the He II line at 2511A. would need 5 eV.

so the energy needed per ion-pair would be about 44 eV.

Assuming the extreme conditions of 100% ionization and excitation at a pressure of  $p$  mm.Hg. the energy needed per c.c. would be

$$(p/760) (6 \times 10^{23}/22400) .44 (1.6 \times 10^{-19}) = \text{about } 0.2p \text{ joules/cc.}$$

The oscillator output was expected to be 100 kW. and it

was hope to concentrate at least 30 KW. of this into a smaller volume of gas Vcc. so during the r.f. pulse there would be

$$(20,000/V) \cdot 10^{-6} \text{ joules/cc./microsec. available.}$$

Equating the power available to the power required shows that the condition for such a discharge would be

$$pV = 0.1 \text{ mm. Hg. cc.}$$

Therefore if 20 KW. could be concentrated into about 1 cc. of gas at about 0.1 mm. Hg. pressure its temperature could be raised to 10,000°K. in a microsecond and maintained there for the whole of the 20 microsec. pulse.

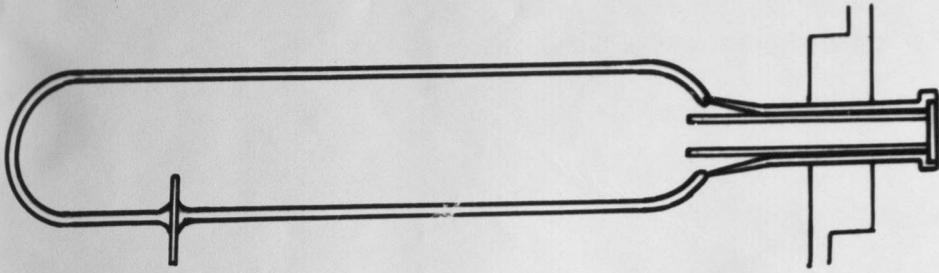
A likely difficulty at low pressures was that a considerable proportion of the gas would be lost owing to "clean up", i.e., owing to adsorption on the walls of the discharge tube.

### (10.3) Power Supply.

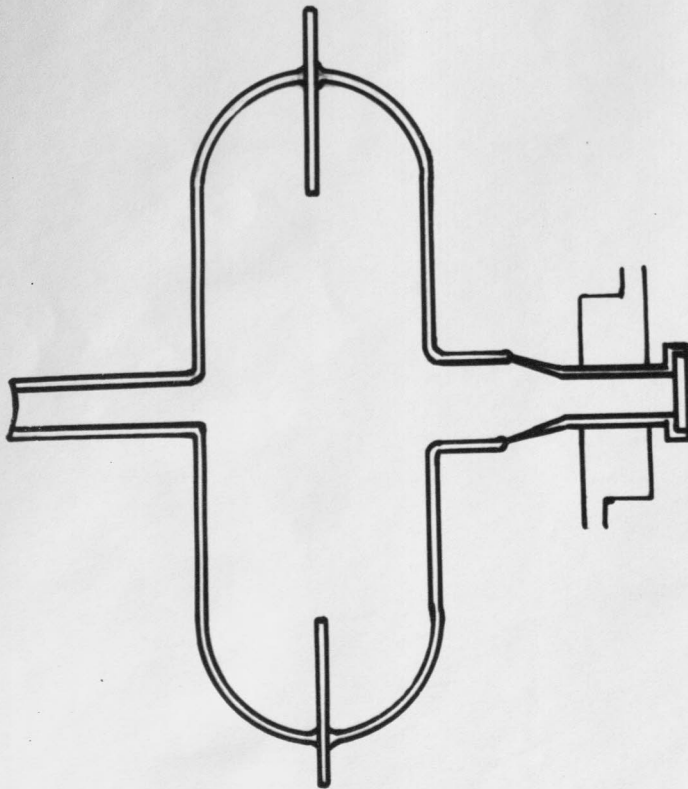
An r.f. discharge was used because of its advantages over a d.c. one for this type of work. Its advantages of greater efficiency at low pressures, more uniform ionization, and less sputtering, have been discussed in chapter 2. Following from the first of these, it is also known to enhance the lines of ionized atoms because its electrons can gather the necessary excitation energy over many half cycles.

The discharge was pulsed in order to run it at high power. The 20 microsec. pulse length was of the order of 3000 cycles of the r.f.; this was expected to be long

enough for a steady state to be reached for the main energy balance in the r.f. discharge (chapter 2), but not for secondary processes such as the formation of metastable ions (Biondi 1951).



2A. FIRST TUBE.



2B. SECOND TUBE.

## 11. PRELIMINARY EXPERIMENTS WITH PULSED D.C. DISCHARGES.

### (12.1) Arrangement of Apparatus.

These experiments showed that fast plates would have to be used, and that 'clean up' would be a serious problem at low pressures.

The first tube used is shown in 2A; it had a tungsten rod anode and a tubular copper cathode which also carried the quartz window. The power supply was the artificial line C described in 4a, which provided a 2.5 m.sec. pulse at 5 K.V. The tube was filled with helium at 0.18 mm.Hg. pressure. After an exposure totalling 54 secs. the helium had so "cleaned up" that it would not break down at 5 kV. and heavy sputtering of the copper cathode had obscured the window. To avoid sputtering, the window of the second tube (2B) looked perpendicular to the discharge, which was between tungsten electrodes. The tube was run in series with the solenoid A described in 4a so that voltages up to 25 KV. could be put across it. It was filled with helium at 0.29 mm.Hg. pressure and run at 8 kV. but 'cleaned up' and after an exposure totalling 50 secs. not even 25 kV. could break it down. It was refilled at 2 mm.Hg. pressure and ran satisfactorily for an exposure totalling 220 seconds. Photographs were taken on Ilford 'Zenith' plates; the first exposure showed only impurity lines; the second showed a few faint He I lines as well but no He II lines. They were anode-pulsed and operated under 'clean C' conditions with up to 10 kV. anode voltage and -1 kV. cathode voltage.

## 12. APPARATUS FOR EXPERIMENTS WITH R.F. DISCHARGES.

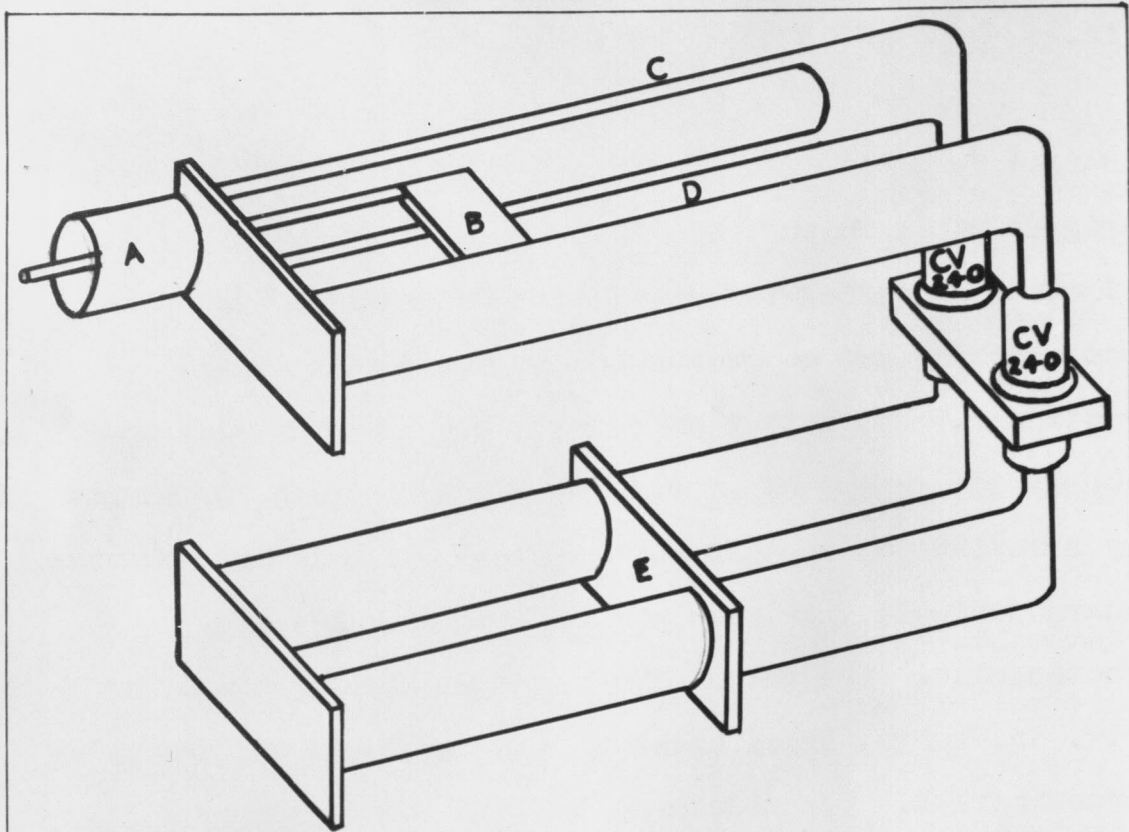
### (12.1) Arrangements of Apparatus.

A rectifier set supplying up to 150 mA. at 20 kV. charged up an artificial line. This was discharged by a trigger pulse which was synchronized to the mains so that it occurred during the half cycle in which the line was not charging and so avoided producing X-rays in the rectifier. The output pulse from the line was used to supply the anodes of an r.f. oscillator, which was shunted by a resistance so that the line and its load had the same characteristic impedance and the output pulse was rectangular. The output from the oscillator pulsed the r.f. discharge, whose spectrum was examined with the prism spectrograph. The discharge tube was made part of a circulating system in which gas which was continuously being circulated and purified replaced that which was lost by 'clean up' in the discharge tube.

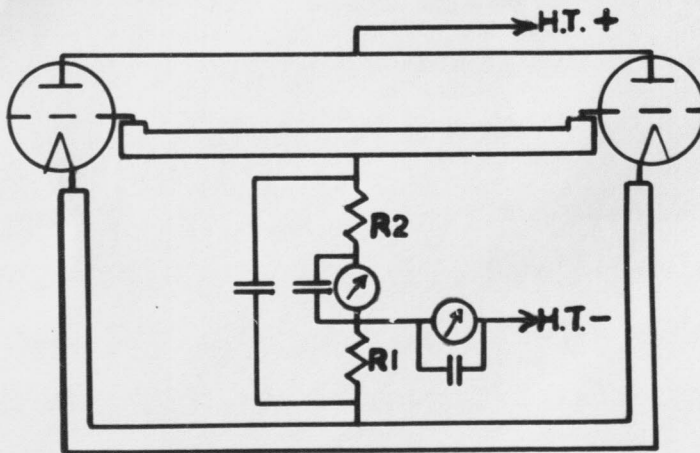
The various pieces of apparatus are described in more detail in the following paragraphs.

### (12.2) The Oscillator.

The oscillator was designed by Professor Sayers and was built in the departmental workshop. Its construction is shown in diagram 3A. Two C.V. 240 triodes were used in push-pull in a tuned-grid, tuned-cathode circuit. They were anode-pulsed and operated under 'Class C' conditions with up to 10 kV. anode voltage and -1 kV. grid bias.



3A. OSCILLATOR.

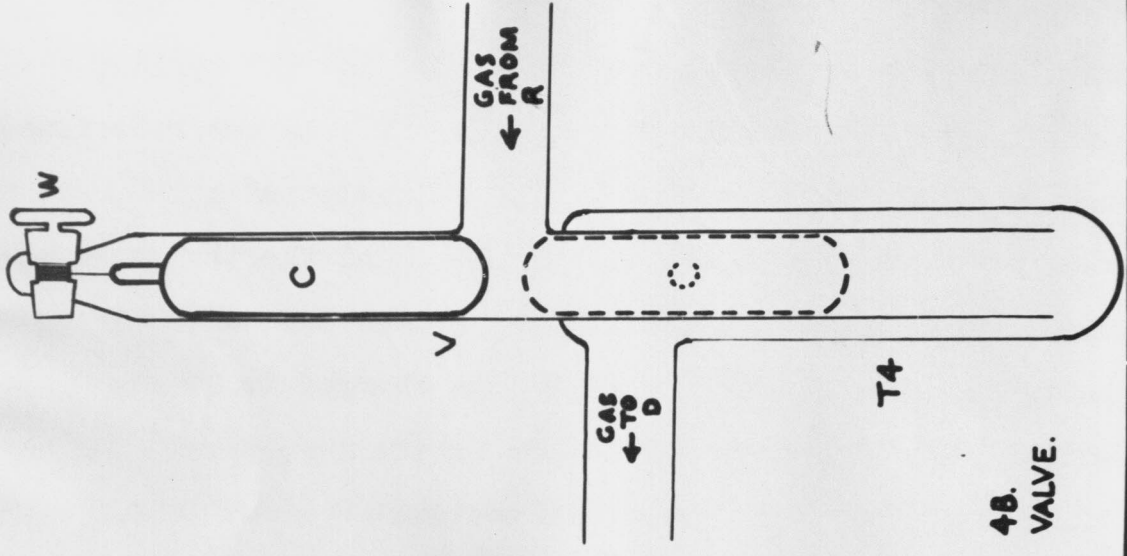


3B. D.C. CIRCUIT.

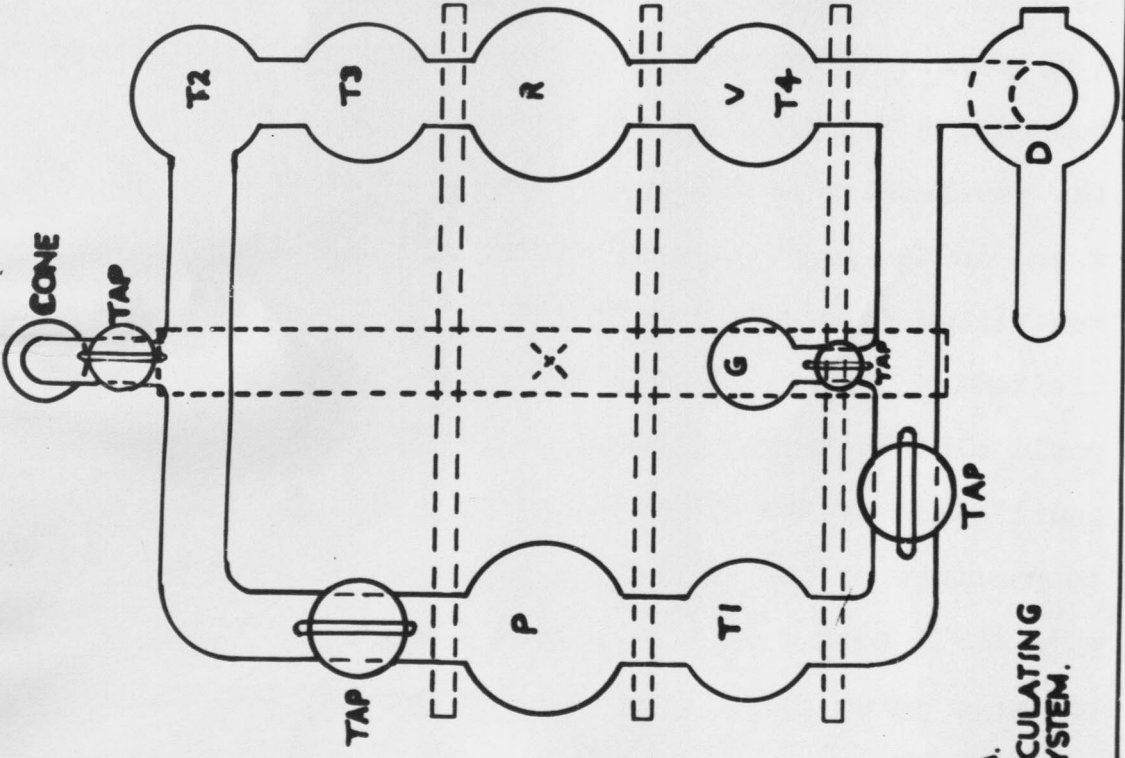
The filament leads were screened from r.f. and the whole oscillator was contained in a metal screening box with separate compartments for cathode and grid circuits. The valves were cooled by air blast. The cathode line was directly coupled to the coaxial output line (A) by means of a sliding inner conductor carrying a bar (B) which projected through a slot running the length of one tube (C) of the cathode line and made spring-loaded contact with the other tube (D). A 'Tufnol' rod (not shown) joined to B projected through the box so that the operator could vary the position of B from outside. The position of the movable short-circuiting bar (E) of the grid line could be varied by similar means. By varying the positions of B and E the oscillator could be matched to its load and also its wavelength could be varied.

The d.c. circuit, diagram 3B, shows how grid bias was provided. The cathode bias resistance  $R_1$ , ensured operation in 'Class A' conditions in the initial period of build up of oscillations; then grid current flowing through both  $R_1$  and  $R_2$  provided further bias so that the valves operated under 'Class C' conditions.

R.f. oscillators are generally run with a pulse length of one or two microseconds and a repetition frequency of about 500 per second. In order to allow the gas discharge load to have more time to reach a steady state this oscillator was designed to have a pulse length of twenty microseconds, and a pulse repetition frequency of 50 per



4B.  
VALVE.



4A.  
CIRCULATING  
SYSTEM.

wavemeter and found to be tunable over the range 180 to 230 cms. by varying the position of B on the cathode line. and of E on the grid line.

The power output was measured calorimetrically. The first measurements were made with the oscillator coupled to a dummy load consisting of a carbon resistance immersed in the water of the calorimeter, and bias resistances  $R_1$  and  $R_2$  were changed until the efficiency was a maximum. The maximum efficiency obtained with either a 25 ohm or 5 ohm (d.c. value) load was  $45\% \pm 2\%$  for  $R_1 = 25$  ohms and  $R_2 = 100$  ohms. The load was then changed to a discharge tube which was surrounded for most of its length by a continuous flow (440 cc/min.) calorimeter which had been previously calibrated using a heating coil of similar dimensions to the discharge tube. The tube contained air at  $10^{-2}$  mm.Hg. pressure and was more difficult to match to the oscillator than the dummy load had been. However, although the calorimetric measurements showed that the efficiency was only 15% with that particular discharge, they also showed that it was possible to get 25 kW. pulses into the gas without overloading the oscillator and this was judged to be sufficient for the purpose.

### (12.3) The Gas Circulating System.

The system is shown in diagram 4A. The gas was circulated by a two-stage mercury diffusion pump P through reservoir R, valve V, discharge tube D and back to the pump. Traps  $T_1$  and  $T_2$  were immersed in liquid air to

keep mercury from the discharge tube; trap T<sub>3</sub> was filled with activated charcoal and was also immersed in liquid air so that other impurities would be removed from the helium as it was circulating. The valve V is shown in diagram 4B from which it is clear that the rate of flow of gas from R to D, and therefore the pressure in D, could be reduced by lowering the glass cylinder C which was attached by a cotton thread to the winch W. It was found essential to make C a very close fit inside the tubing in order to cover a wide range of pressure. The pressure in the system was measured with a Pirani gauge, G. This was unfortunately made of soda glass and had to be connected to the system by a cone and socket, therefore in order to prevent grease vapour from this entering the discharge the gauge was put downstream from the discharge tube. The makers supplied a set of calibration curves which enabled the gauge to be used for various gases, including helium, without further calibration. The difference of pressure between the discharge tube and the gauge was calculated (from a formula given by Dushman) to be less than  $10^{-3}$  mm.Hg. for the experimental conditions. The pressure of the discharge could be varied from 1 mm.Hg. with the valve fully open to  $2 \times 10^{-2}$  mm.Hg. with the valve fully closed. The only grease between the activated charcoal in trap T<sub>3</sub> and the discharge tube D was that on the winch W (which was made from a glass tap); lest this grease vapour should prove troublesome in the discharge the valve V was joined directly to trap T<sub>4</sub>,

which could be surrounded by liquid air if it were necessary.

The system was mounted on a duralumin frame (shown dotted in diagram 4A) consisting of a central torsion-bar through which were driven square rods to take the weight of the glass components. The system was suspended from a retort stand by a coil spring attached to the duralumin frame near to the centre of gravity (x) so that it could be connected either to the pumping train for filling with gas, or to the oscillator for running the discharge, without undue risk of breakage.

When the discharge tube was run at pressures of the order of a mm.Hg. the discharge filled the whole system. The blue colour of the mercury discharge was clearly confined between traps  $T_1$  and  $T_2$ , however, there were always mercury lines in the spectrum photographs as was to be expected since the mean free path for mercury was only about 0.2 cm. even at the lowest pressure used (0.03 mm.Hg) and the traps were of more than 1 cm. diameter.

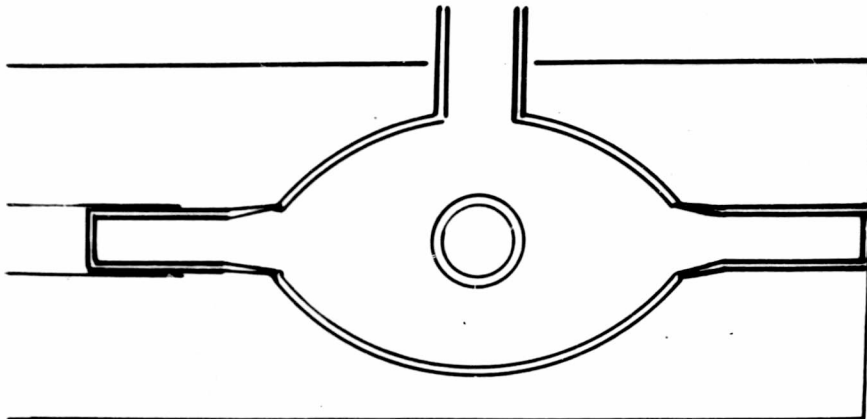
#### (12.4) Spectroscopic Apparatus.

A Hilger Littrow large quartz prism spectrograph was used to photograph the spectra. Two condensing lenses were used. A condenser of long focal length placed close to the slit of the spectrograph was used to illuminate the slit uniformly along its length and form an image of the discharge at the collimator lens, then by putting a known step-filter directly in front of the slit each plate could

be calibrated for variation of photographic blackening with intensity of light. A slit width of 0.05 mm. was used for this since only the peaks of the lines were needed for the calibration. The long focus lens was too slow to be used with the narrow slit (0.005 to 0.015 mm.) needed for the measurement of line breadths; so for that purpose it was replaced by a lens of shorter focal length and smaller f number, which formed an image of the discharge at the slit. The line contours were plotted using a Hilger non-recording photo-electric microphotometer in the Department of Physics. The ratio of the steps of the filter was known for visible light but not for ultra-violet. An attempt was made to calibrate the filter by using an absorption spectrophotometer over the wavelength range used in the experiment. This was unsuccessful because when the instruments' beam had been reduced sufficiently in area (by about 1000:1) to examine one step of the filter, its photocell could not respond to it.

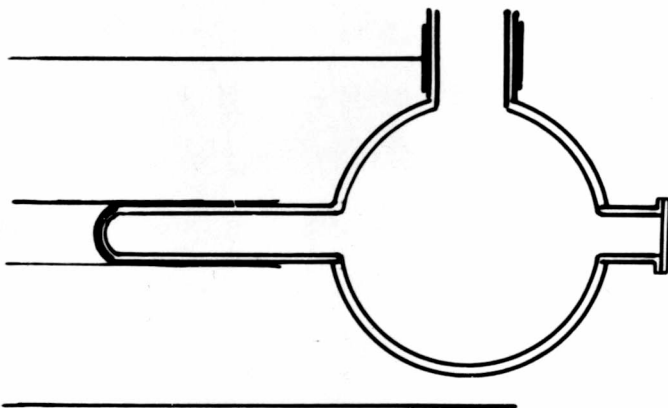
(12.5) Discharge Tubes.

Four types of tube were tried; these are shown in 5A, B, C, D. All were made to fit the coaxial output line of the oscillator and all were joined to the gas circulating system by a side arm shown in the diagram; in B, C and D the window looked along the discharge, in A it was on another side arm. Types A and B were unsatisfactory, C was partially satisfactory, D was successful. "Araldite"



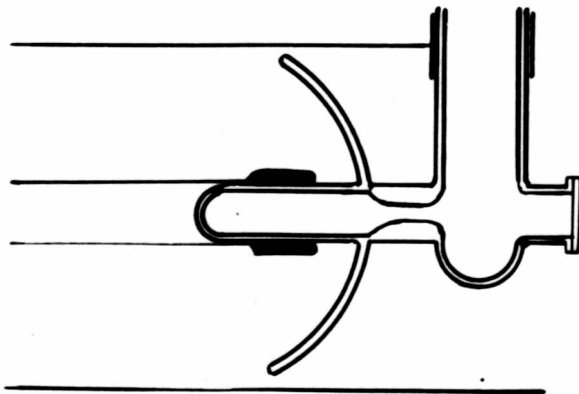
TUBE A

5A.



TUBE B

5B.



TUBE C

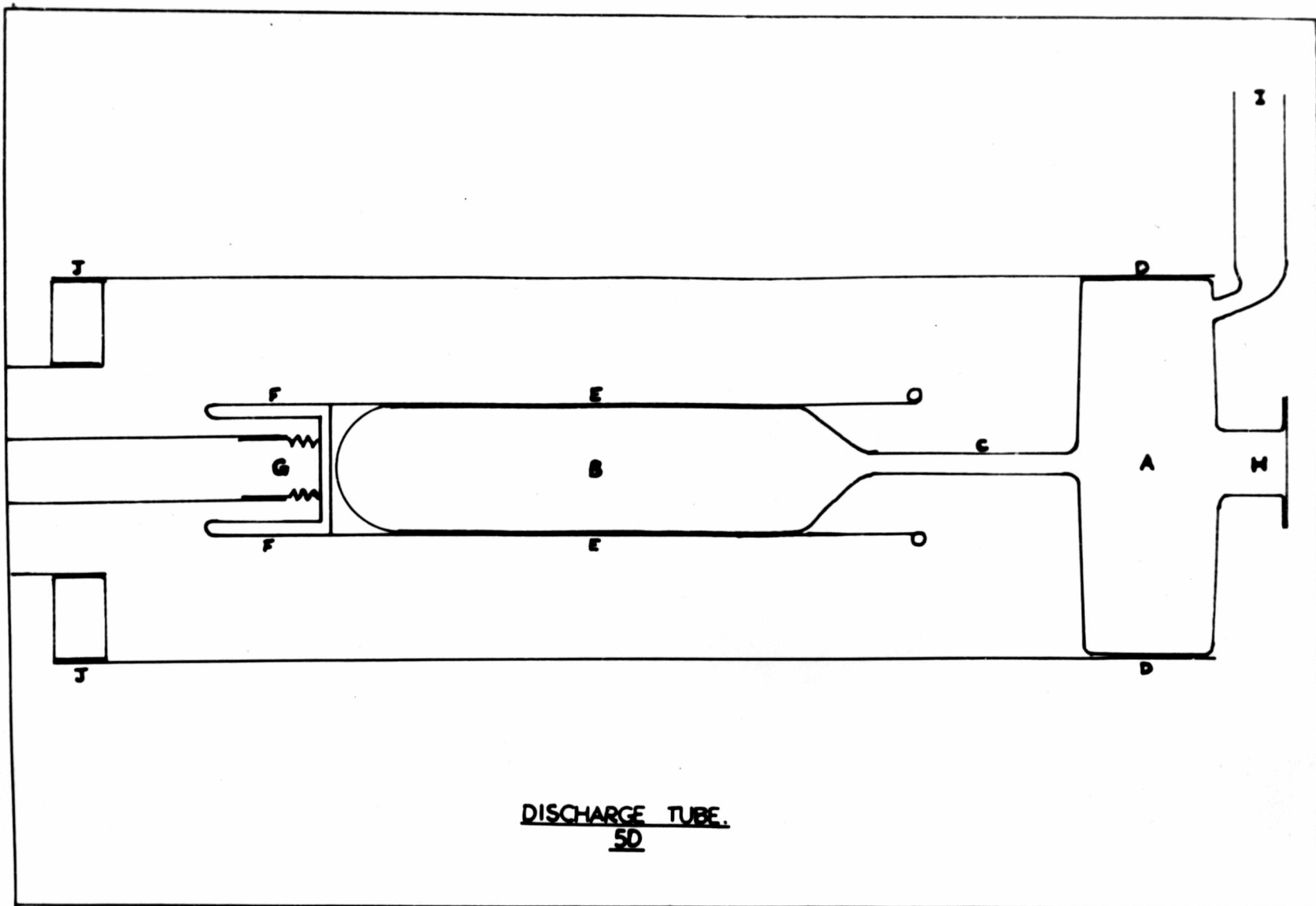
5C.

was better than silicone varnish as a cement for the window.

Type A: had copper-to-glass seal electrodes for low impedance; these seals could not be cleaned properly and they sputtered badly. No lines of He II appeared on the spectrum photographs.

Type B: avoided A's defects by being electrodeless but suffered from severe sparking where the glass slid into the inner conductor of the output line; again, no He II lines appeared in the spectrum.

Type C: was silvered to make good contact where it joined the inner conductor, also had a corona shield and had a matching stub inserted between it and the oscillator; these measures did not prevent sparking when the pressure was below the order of  $10^{-1}$  mm.Hg. The constriction in this tube was designed to concentrate the r.f. power into a small volume of gas in the hope of exciting the He II spectrum. In this it was successful. Photographs taken with the fast lens showed the usual long lines of He I and Hg (from the pump) which were therefore excited in the whole tube, and also short lines of He II at 3203A and 2733A. which were therefore excited only in the constriction. There were also short lines of Si (except 2882A which was long) showing that the power in the constriction was sufficient to sputter the glass (there were no silicone compounds in the vacuum system). Most of the work of chapter 13 was done with this tube; eventually the sparking at low pressure so de-vitrified the glass that it cracked



DISCHARGE TUBE.  
50

off at the edge of the inner conductor of the output line.

Type D: This tube was also constricted but had electrodes of large area to reduce the impedance between the electrodes and the gas and thus reduce the chance of sparks tracking along the surface of the glass. There was no trouble with sparking, even without a matching stub in the output line, and the discharge could be run at pressures as low as  $10^{-2}$  mm.Hg. At the lowest pressures the luminosity was very feeble and could probably have been increased if a good matching device had been available (e.g. a double stub) to match the tube better to the line.

This was the tube which was used in the main experiments; it is shown in diagram 5D. The inner and outer conductors of the output line were stepped up in diameter from  $\frac{1}{2}$ " to 1" and from  $1\frac{1}{2}$ " to  $2\frac{3}{4}$ " respectively, thus keeping the characteristic impedance about the same, and the electrodes were connected to parts A and B of the tube, each of which had an area of about 10 sq.ins. A fitted tightly into a thin flexible copper outer conductor D. B fitted closely inside a thin copper sleeve E on the end of cylinder F, which was in turn connected via bellows and a short tube G to the  $\frac{1}{2}$ " dia. inner conductor. This arrangement saved the tube from mechanical strain. The sharp edges of G and of the bellows were shielded by F, and both the end of F and the end of E were rounded to prevent sparking from them. The quartz window H was fixed with cold-

setting 'Araldite' to a ground glass flange, Tube I was sealed to the gas-circulating system. The discharge tube and its electrodes were built into one unit which was easily connected to the oscillator's output line at G and J. *ation.*

Constriction C was about 0.3 cm. diameter and 4 cm. long. Most of the high temperature helium atoms would stay inside it since even at the lowest pressure used (0.033 mm. Hg.) their mean free path would be only about 1 cm. (0.7 cm. at 300°K., increasing only slowly with temperature) and only a fraction  $1/e$  would have a path length greater than the mean. C was not made longer than a few cm. because atoms which travelled at an angle to its axis would be reflected from its walls with a velocity distribution which depended on the wall temperature and the accommodation coefficient (see 9.3) rather than on the gas temperature alone, so tending to increase the number of atoms with low components of velocity in the axial line of sight and making the line-contour appear broader in the wings and narrower in half-intensity breadth. In practice, this effect on the contour was less important than broadening by Stark effect. The collisions of the electrons (mean free path about 5.6 times that of atoms) with the walls appears to have had an adverse effect on a later attempt to measure the excitation temperature (17.2).

The solid angle subtended by C at H could have been increased by making A concave towards C; also, the

power input to C could have been measured by constant-flow calorimetry if it had been surrounded by a water-

(13.1) Summary. However, neither of these modifications were used

because of shortages of time and difficulty of construction. Subsidiary experiments, which were performed to find out how much instrumental effects altered the breadth of spectrum lines on the photographic plate, showed the following.

- (13.2) The variation in temperature of the spectrograph proved to be very important.
- (13.3) The focus of the collimator of the spectrograph was not critical.
- (13.4) The width of the spectrograph slit was important.
- (13.5) The width of the microphotometer slit was not critical.
- (13.6) The grain of the photographic plate was not important.
- (13.7) The instrumental line contour was found to be approximately gaussian.
- (13.2) The variation in the temperature of the spectrograph.

A change of spectrograph temperature causes broadening of the spectral lines and changes in focus, because the refractive index of the quartz parts and the dimensions of the metal parts change.

The displacements of a line of wavelength  $\lambda$  due to change of the refractive index  $n_{\text{ord.}}$  of the quartz prism with temperature  $T$  was estimated as follows:-

$$\text{at } 2500\text{\AA.}, \quad dn/dT = -1.66 \times 10^{-6}/^{\circ}\text{C},$$

$$\text{and} \quad dn/dl = 6.35 \times 10^{-5}/\text{\AA}$$

### 13. INSTRUMENTAL EFFECTS.

#### (13.1) Summary.

Subsidiary experiments, which were performed to find out how much instrumental effects altered the breadth of spectrum lines on the photographic plate, showed the following.

(13.2) The variation in temperature of the spectrograph was proved to be very important.

(13.3) The focus of the collimator of the spectrograph was not critical.

(13.4) The width of the spectrograph slit was important.

(13.5) The width of the microphotometer slit was not length critical.

(13.6) The grain of the photographic plate was not angle of important.

(13.7) The instrumental line contour was found to be pencil of approximately Gaussian.

#### (13.2) The variation in the temperature of the spectrograph.

$6.5 \times 10^{-4}$  A change of spectrograph temperature causes the braodening of the spectral lines and changes in focus, because the refractive index of the quartz parts and the dimensions of the metal parts change.

The displacements of a line of wavelength  $\lambda$  due to change of the refractive index  $n_{ord.}$  of the quartz prism with temperature  $T$  was estimated as follows:-

at 2500A.,  $dn/dT = -1.86 \times 10^{-6}/^{\circ}C$ ,  
and  $dn/d\lambda = 6.25 \times 10^{-5}/\text{A}$

$$\left. \begin{aligned} dl/dT &= (dn/dT) / (dn/dl) = 3 \times 10^{-2} \text{A}/^\circ\text{C} \text{ at } 2500\text{A} \\ \text{Similarly } dl/dT &= 8.4 \times 10^{-2} \text{A}/^\circ\text{C} \text{ at } 3000\text{A} \end{aligned} \right\} (13A)$$

The change in focal length  $f$  of the quartz lens was estimated from the formula for a thin lens

$$1/f = (n - 1)(1/r_1 - 1/r_2) \quad (13B)$$

$$\text{from which } \frac{df}{dT} = \frac{-1}{(n-1)^2 (1/r_1 - 1/r_2)} \cdot \frac{dn}{dT} = \frac{-f}{n-1} \cdot \frac{dn}{dT} \quad (13C)$$

$f$  was 170 cm., at 2500A.  $n = 1.6$  and  $dn/dT = -1.86 \times 10^{-6}/^\circ\text{C}$  so the decrease in  $f$  was only  $5.3 \times 10^{-4}$  cm./ $^\circ\text{C}$ .

The expansion of the 170 cm. of spectrograph bed between the lens and the photographic plate was estimated at  $2.2 \times 10^{-3}$  cm./ $^\circ\text{C}$ ., which added to the change in focal value for 3000A. length would cause the plate to be out of focus by  $2.7 \times 10^{-3}$  cm./ $^\circ\text{C}$ . The lens was 7.5 cm. diameter, so subtended an angle of  $\tan^{-1}(7.5/170)$ , and the plate was inclined about  $30^\circ$  to the optical axis, therefore the diameter of the pencil of light at the plate would be:  $(7.5/170)(2.7 \times 10^{-3}) \text{ cosec } 30^\circ = 2.4 \times 10^{-4}$  cm./ $^\circ\text{C}$  which corresponds to only  $6.5 \times 10^{-4}$  A/ $^\circ\text{C}$  at 2500 A. and is small compared with the effect of the prism (13A).

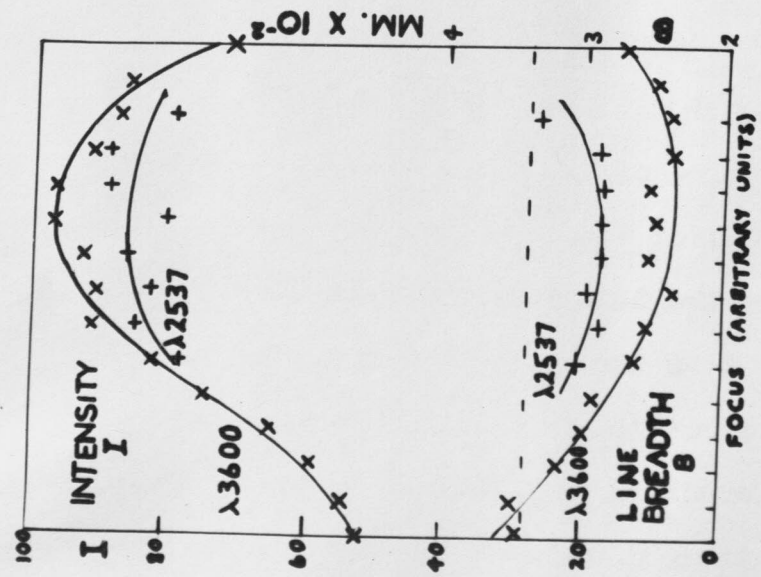
The following experiment was carried out to measure the displacement of a line. The temperature of the spectrograph was measured to  $0.05^\circ\text{C}$ . by a mercury thermometer whose bulb pressed closely against the metal case of the spectrograph, but was lagged from the surrounding air. The spectrum of a neon bulb was photographed; this took only

ten minutes during which time the spectrograph temperature never changed more than  $0.1^{\circ}\text{C}$ . The spectrograph was left completely undisturbed for several hours while the temperature was allowed to drift several  $^{\circ}\text{C}$ , then the spectrum was photographed again on the same portion of the plate. Each line in the spectrum appeared as a 'doublet' whose separation was due to the change in temperature. The distance between the peaks of the 'doublets' of shortest wavelength was measured on the microphotometer; owing to the neon bulb having a glass envelope the shortest wavelengths were 2968, 3022, 3024A. of a Hg. impurity. The mean displacement was  $15 \times 10^{-2} \text{A./}^{\circ}\text{C}$ , almost twice the calculated value for 3000A. It was reasonable to conclude that the displacement at 2500A would therefore be approximately  $6 \times 10^{-2} \text{A./}^{\circ}\text{C}$ , rather than  $3 \times 10^{-2} \text{A./}^{\circ}\text{C}$  as calculated.

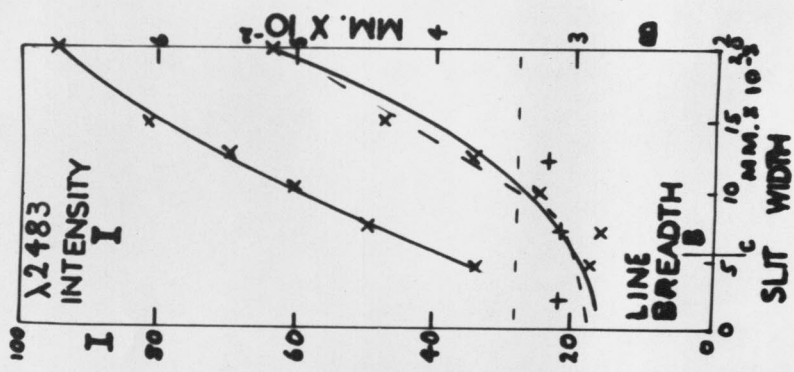
Since the Doppler broadening for  $10^4 \text{ }^{\circ}\text{K}$  at 2500A. was only  $9 \times 10^{-2} \text{A}$ . it was clearly necessary to keep the temperature of the spectrograph as steady as possible during exposures of the discharge spectrum. This was attempted by keeping the laboratory temperature at a constant value higher than the maximum daily room temperature by means of 3 kW. electric fires under the control of a thermostat with a differential of  $0.25^{\circ}\text{C}$ . A box built round it and its own large thermal capacity helped to protect the spectrograph from sudden fluctuations in temperature and fans were used to reduce the temperature gradients in the room.

INSTRUMENTAL EFFECTS: SPECTROGRAPH.

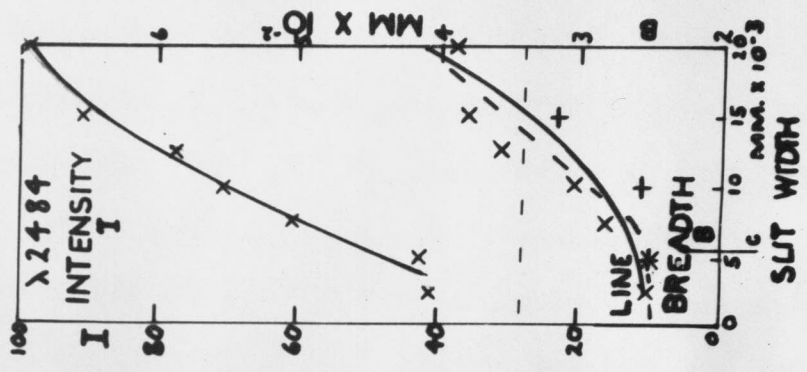
6 A.



6B.



6C.



-- DOPPLER BREADTH,  $10^4$  K,  $\lambda 2511$ .

(13.3) The focus of the collimator.

Photographs were taken of a neon bulb spectrum for various settings of the focus of the collimator. The contours of the neon line at 3600A. were plotted using the microphotometer and converting its galvanometer deflection to relative intensity (as described in chapter 15). The line breadths were measured graphically, and it was found that they did not vary greatly with focus; however the collimator was of course set to the best focus. Later on this experiment was repeated for the actual discharge tube using the mercury line at 2537A. and the result was confirmed. The results for both wavelengths are shown graphically in 6A. The dotted line shows the Doppler breadth at  $10^4$ °K and 2511A.

(13.4) The width of the spectrograph slit.

The effect of slit width on the peak intensity and the half-intensity-breadth of spectrum lines has been shown in 6B and 6C. The variation of the peak intensity and the half-intensity-breadth of spectrum lines has been treated theoretically by various authors, but complete agreement is lacking and attempts to check the theories whether or no there were a sudden change have been inconclusive. It is generally agreed that there is a critical slit width  $c$  and that

$$c = (\text{f-number of collimator lens}) \times (\text{wavelength used}) \quad (13D)$$

As the slit width is increased from infinitely narrow to the critical width the peak intensity rises rapidly but the breadth increases only slightly. For wider slits the peak intensity rises more slowly but the breadth rises linearly,

being directly proportional to the slit width.

From 13D the critical slit width for 2500A. with the spectrograph used ( $f = 22.7$ ) was  $6 \times 10^{-3}$ mm. An experiment was done to check this under conditions as near as possible to those of the main experiment; unfortunately, the control for varying the slit width was calibrated in steps of  $5 \times 10^{-3}$ mm. and could not be set accurately to a fraction of a step. It was impracticable to do the experiment with the line at 2511A. from the actual discharge tube because this line was very difficult to obtain. Instead, a low pressure mercury in quartz discharge was used with same arrangement of condensing lens as for the discharge tube; the only difference was that it was an extended source (about  $100 \text{ cm}^2$  instead of  $4 \text{ cm}^2$ ). Exposures of 100 seconds were ample. The mercury lines at 2483 and 2484A. were studied with the microphotometer, and the variation of the peak intensity and half-breadth is shown in 6B and 6C.

The scatter of the points was too great to say whether or no there were a sudden change in the slope of the half-breadth v. slit width curve, but there certainly was an increase in slope with slit width which was greatest in the region of the calculated critical slit width (c). The graphs of intensity v. slit width seemed however to show that the intensity continued to rise rapidly up to about three times the calculated critical slit width. The Doppler broadening expected at  $10^4 \text{ }^\circ\text{K}$  for 2511A. is shown

on the graphs for comparison with the rest of the data. Dotted curves are also drawn to show how the half breadth results might be interpreted to agree with theoretical requirement of a sudden change in slope, but this cannot be said to be either verified or disproved because of the scatter of the experimental points.

The random error in the measurement of the half breadth appears from 6B and 6C to have been about  $\pm 20\%$ . Within such limits it was not possible to detect any change of line breadth over the wavelength range 2480-3030A., (graph 9B).

(13.5) The width of the microphotometer slit.

Various lines were scanned with photocell slit widths varying up to one sixth of the half-intensity-breadth of the line and four times the spectrograph slit width. Within this range the width of the photocell slit did not affect the line breadth.

(13.6) The grain of the photographic plate.

Even the largest grains would not be expected to be larger than about  $10^{-3}$  cm., and it was estimated by examining a developed plate under a microscope that the average grain size was of the order of not more than a twentieth of the half breadth. In using the microphotometer at least 1 mm. length of line was always used so the effect of the grain would be averaged out; this was confirmed by the fact that the microphotometer readings invariably gave a smooth line contour. Ilford 'Zenith' plates were used.

All the plates were developed in 'Promicrol' fine grain developer which is said to increase the effective speed of the plate. the charcoal was baked to out-gas it.

(13.7) The instrumental line contour. Isolated by closing

If instrumental broadening by itself produced a Gaussian line contour of half breadth  $b_1$ , and Doppler broadening by itself produced a Gaussian contour of half breadth  $b$ , then their resultant contour would also be Gaussian and would have half breadth  $b_2$  where, in units of  $\text{cm.}^{-1}$  (Allen 1932).

$$b_2^2 = b^2 + b_1^2 \quad (13E)$$

Consequently,  $b$  could be deduced from measurements of  $b_1$  and  $b_2$ . For accuracy in the main experiment the spectrograph slit width was kept sufficiently narrow for  $b_1$  not to exceed the expected magnitude of  $b$ . The Doppler broadened contour was expected to be Gaussian (8.1). The instrumental contour was found to be nearly Gaussian, except in the wings, for the neon and mercury lines (2484, 3208, 3600 A.) already studied (13.3, 13.4); these lines had been emitted from relatively cool sources and so  $b$  had been negligible compared with  $b_1$ . Plots of the log. of the intensity against the square of the width of the contour (10.1) did not deviate from linearity until the intensity had fallen to less than 20% of its peak value (curves "I" in figs 12 and 13).

later. The walls were bombarded with neon instead of helium because it was easier to see the colour change with contamination; and although

14. EXPERIMENTAL PROCEDURE.

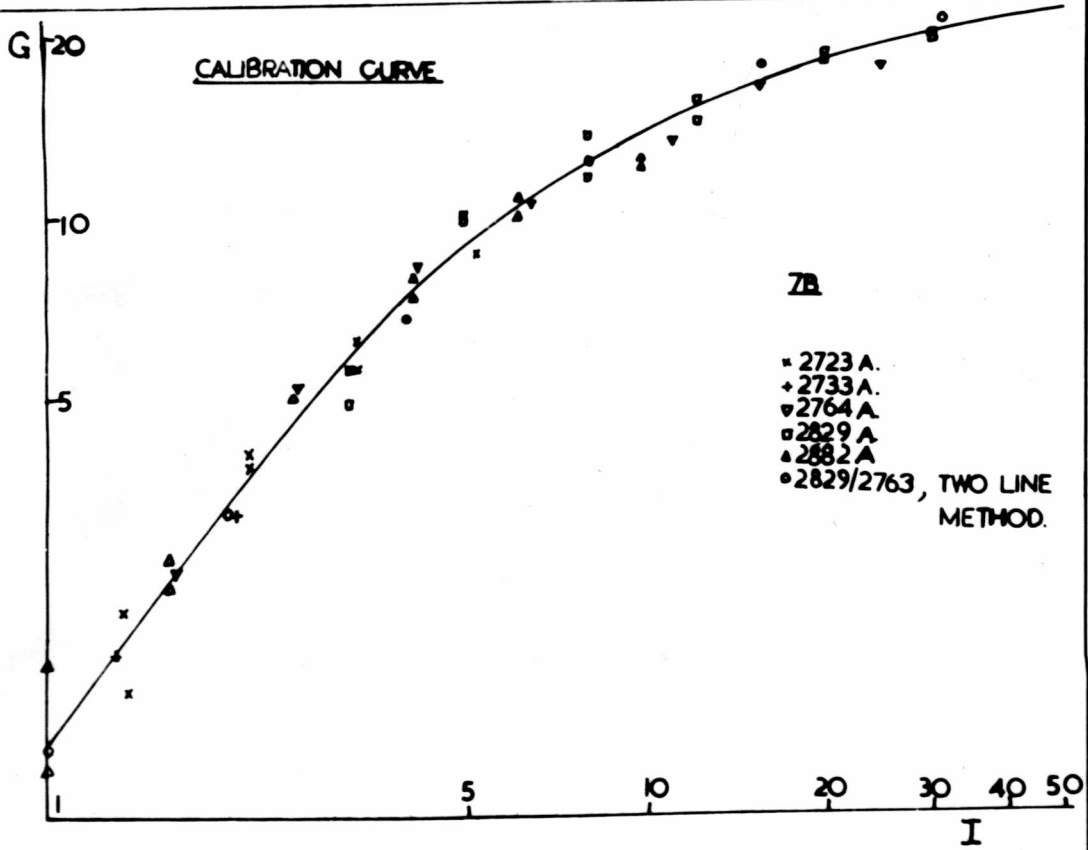
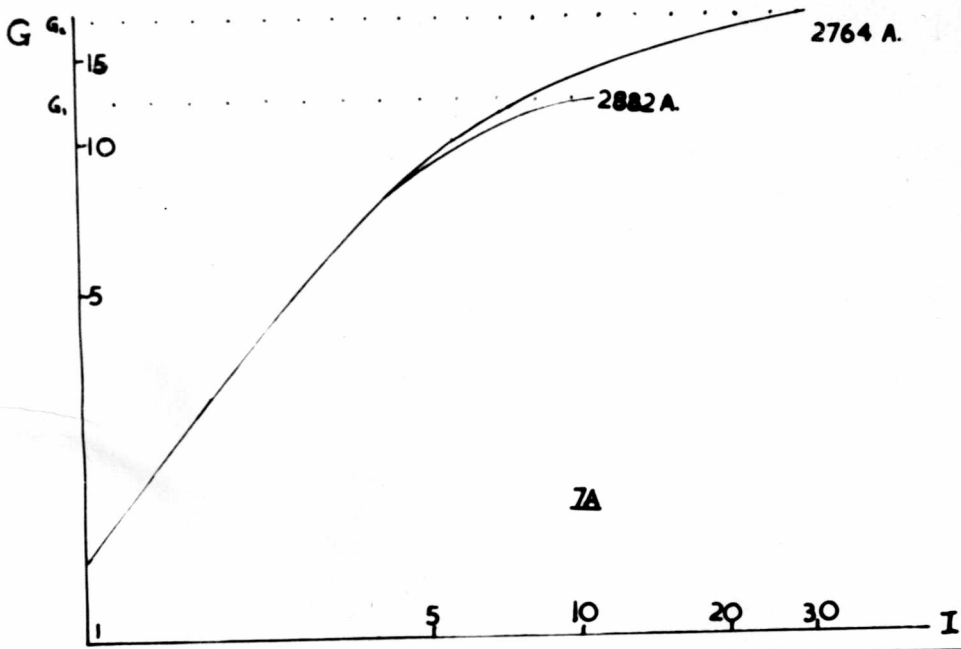
(14.1) The gas circulating system was evacuated and at the same time the charcoal was baked to out-gas it. The pump of the circulating system was isolated by closing the appropriate taps and the rest of the system was filled with neon at about 1 mm.Hg. pressure. Copper foil electrodes were wrapped round the discharge tube and the rest of the neon-filled section at intervals of a few inches and were connected alternatively to opposite sides of the coil of the Department's 100 Kc. r.f. heater. (The heater was used at power '2', the coil was water cooled, and the power was switched on for three minute intervals, with three minute rests between each interval lest a hole should be burned in the glass). Gases such as air, water vapour and carbon dioxide which were driven out of the glass by the ionic bombardment changed the colour of the neon discharge from red to bluish. After about thirty minutes the bombardment the section was refilled with clean neon and this process was repeated until the discharge stayed the colour of clean neon; this took about six hours bombardment. When the glass had been so cleaned the neon was pumped out, liquid air was put round all the traps, and the entire circulating system was filled with helium at the required pressure. The system was then removed from the pumping train and connected to the oscillator. The walls were bombarded with neon instead of helium because it was easier to see the colour change with contamination; and although

it was necessary to avoid band spectra, it was not necessary to avoid neon lines because they did not fall near the helium line studied.

(14.2) The thermostatic control for the room was switched on sixteen hours before exposures were begun, in order to allow the prism temperature to become steady, and it was kept on day and night until the exposures had all been finished. For a three hour exposure the indicated change in the daytime was 0.3 to 0.5°C, and in the evening it was about 0.1 to 0.2°C generally being less on clear evenings than on cloudy ones; after midnight the temperature tended to fall again. The oscillator input was 150-200 watts. and it had to be within a metre of the spectrograph. The heat dissipated by it tended to cause a slight rise in spectrograph temperature after switching on, so it was left running for an hour before each exposure was begun. In order to measure the line broadening caused by the temperature drift, the spectrum of a neon bulb was superimposed on the same part of the plate for ten minutes before and ten minutes after the exposure to the discharge spectrum.

(14.3) Exposures of the discharge were for three hours running time which was equivalent to 10.8 secs. continuous exposure (intermittency effect is unimportant for pulses less than 100 microsec.); this was about the longest time for which the temperature drift could be kept small, and

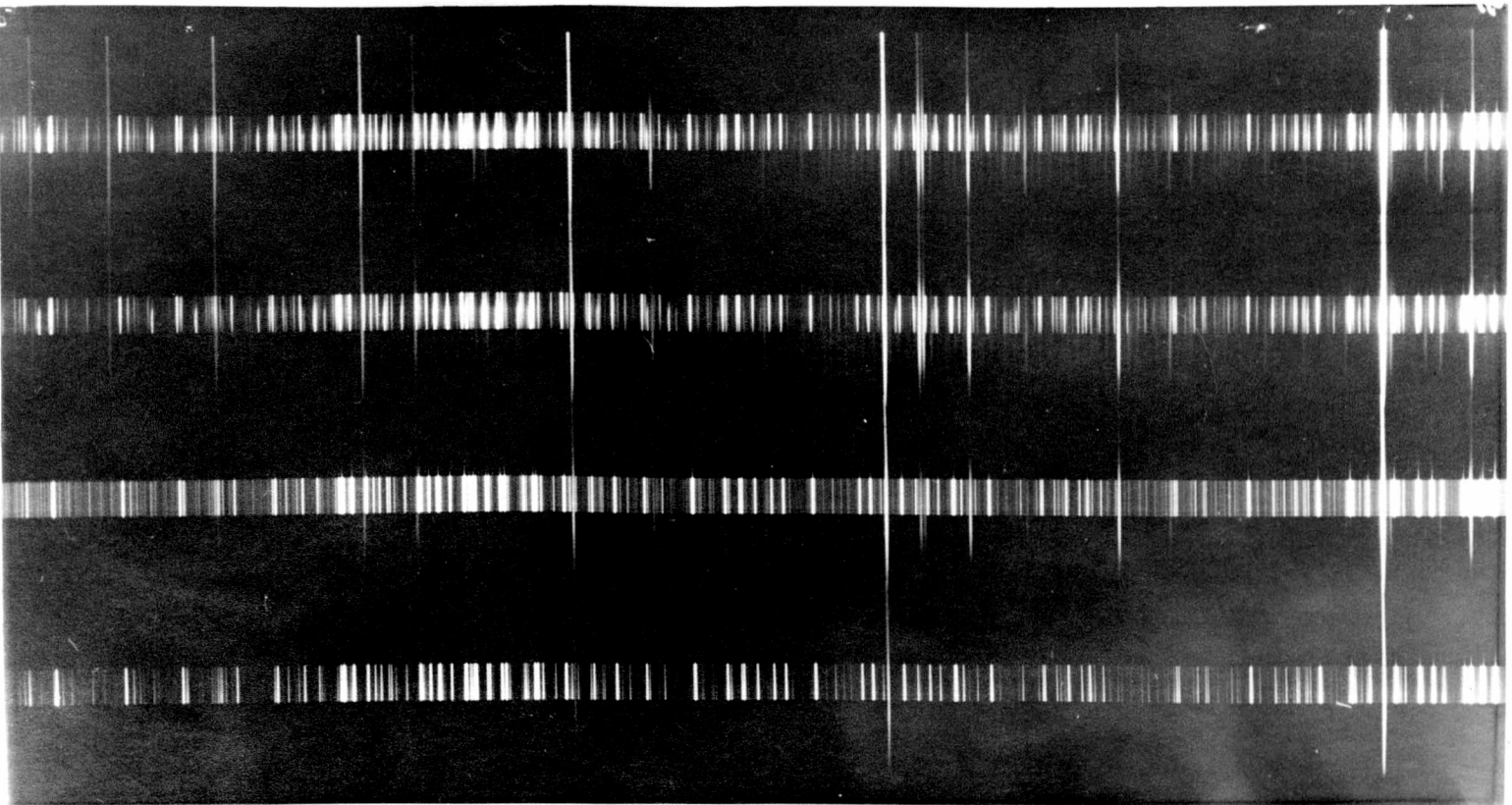
doubling it would have increased the plate blackening by only 30% at the cost of doubling the temperature drift. The results showed later on that the temperature drift had serious effects even in three hours. For the measurement of line breadths the discharge spectra were photographed for three slit-widths up to the maximum that could be used for reasonable accuracy (13.7) i.e. 0.005, 0.010, 0.015 mm.; also for the minimum pressure for a reliable discharge, and two higher ones; 0.033, 0.15 and about 1 mm.Hg. The last pressure was uncertain because the Pirani-gauge head had become unserviceable, but it was the highest obtainable and was certainly not less than 1 mm.Hg. Calibration marks with the seven-step filter, slow lens, and wide slit, were put on the plate during daytime when the temperature drift was too great for the main experiment. A second set of calibration marks were made with the filter inverted to check its uniformity of illumination. Iron arc comparison spectra were also put on the plates. During development the plates were brushed with a soft brush to reduce Eberhard effect and this treatment seems to have been successful for the lines studied (which were not very strong).



plot in 15. THE METHOD OF FINDING THE LINE CONTOURS.

The wavelengths of the lines were found by comparison with the iron arc spectrum, generally this could be done by inspection but the wavelengths of important lines (such as 2511A. of He II) were measured using a travelling microscope. The lines were then scanned with the microphotometer taking the 'clear glass' reading near each particular line. The galvanometer deflection  $G$  was converted to relative intensity  $I$  by plotting a calibration curve from the density marks on the plate. This calibration curve was made by plotting the peak deflections for the seven calibration steps on log-log paper against numbers proportional to the relative intensities of the light beams which had come through the seven calibration steps; the ratios of the intensities were those for visible light, since those for ultra violet light were unknown. The two sets of density marks for each line agreed, thus showing that the filter had been uniformly illuminated. The main lines of interest lay in the range 2723 - 2882A. The curve for a line whose peak calibration deflections ranged up to  $G_1$  was not parallel to the 0 to  $G_1$  region of a stronger line whose peak calibration deflections had ranged up to  $G_2$  (greater than  $G_1$ ) but deviated from it in the region of  $G_1$ , as shown in 7A. This shape of the calibration curve for the weaker lines could not have been a photographic effect because each one deviated at a different value of  $G$ , it must therefore have been caused by having to

plot intensity ratios for visible light instead of for the region 2723-2882A. In view of this the best curve was obtained by displacing that for each line laterally along the log I axis and drawing the mean, and this mean curve, shown in 7B., was used as the calibration curve for that spectral range. The line contours for the helium lines 2723 and 2763A. and the He II line 2733A. were plotted from both the individual calibration curves and the mean one; the average difference in half breadth was less than 3% for 2723 and 2733A., and about 10% for 2764A. The calibration curve deduced by the 'two line method' (Churchill 1944) using the helium lines 2829 and 2764A. gave six points which agreed well for one plate with the mean calibration curve; for the other plate the method gave only three points and was not much use. The mean curve for both plates was the same within the limits of experimental error and the scattering of the points about each curve was also about the same. The calibration curve for the mercury resonance line 2537A. did not fit the mean curve, so the scattering of the points was not so great as the variation in plate calibration over about 300A. in the ultra violet (where it probably varies much more rapidly than in the visible region).



He I, 2945

Sc, 2882

Hg, 2848

CII { 2838  
2837

He I, 2829

Hg, 2537

S, 2528

S, 2524

S, 2519

S, 2516

S, 2514

S, 2512

Cr, 2509

Cr, 2507

He I, 2511

2764

C I } 2498  
Hg } 2479

2723

2723

0.18 mm.Hg.

2696

2677

2663

1 mm.Hg.

0.25 mm.Hg.

0.07 mm.Hg.

0.02 mm.Hg.

16. THE SPECTRA.(16.1) Useful helium lines.

The He II line at 2511 Å. was only just visible even on photographs, such as plate 8, which were taken with a much wider spectrograph slit than could be used for a reliable estimate of Doppler broadening (13.7) and there was no trace of He II lines of shorter wavelength. There were however three He I lines (2723, 2764, 2829Å.) and one He II line (2733Å.) from whose breadth the gas temperature was estimated. The breadth of the He I line at 2945Å, and of the He II line at 3203Å. could not be measured sufficiently accurately because of the smaller dispersion at those wavelengths, and the He I line at 3189Å. was over-exposed. The excitation temperatures for the series were estimated from the relative intensities of all the lines (except 3189) of He I, and both of He II; the equilibrium temperature was estimated from comparison of the two series. The dispersion at the appropriate wavelengths was found from measurements of the iron-arc spectrum which was on the same plate as the helium lines.

(16.2) Effect of the constriction in the discharge tube.

The constriction fulfilled its purpose of concentrating as much power as possible into a small volume

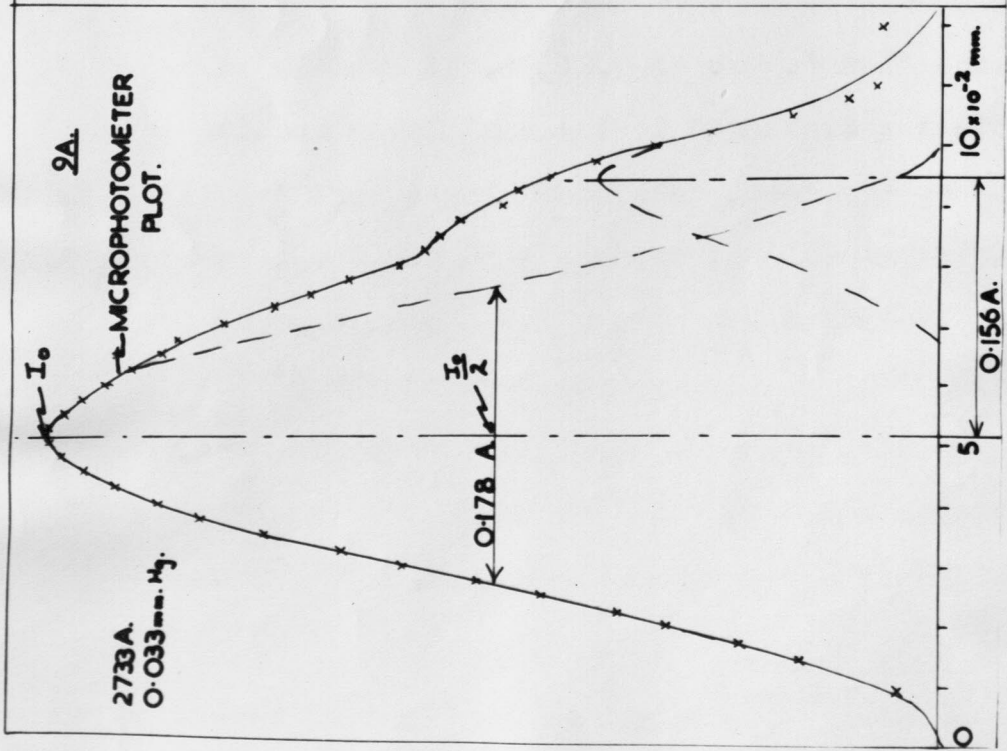
(16.3) Impurities.

This was shown both by the discharge being brightest in the constriction, and by spectrum photographs taken with the condenser of short focal length. These photographs showed both 'long' lines which had been excited

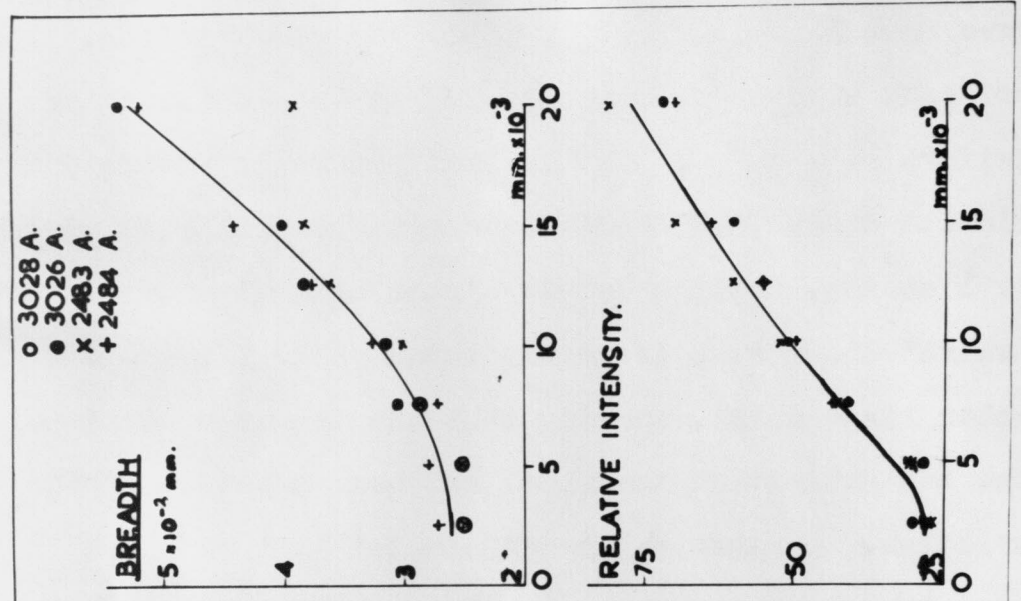
throughout the discharge tube, and 'short lines which had not been appreciably excited outside the constriction. The part of each line which corresponded to the constriction was uniform in density, but the rest generally became fainter towards its ends. The 'long lines were generally those of the He I and Hg. spectra and the 'raie ultime' of Si (2882); the 'short' lines were generally those of He II, C II, and the other lines of Si, showing that the degree of ionization and the bombardment of the glass had been greatest at the constriction. Whether a line appeared 'long' or 'short' depended to some extent upon the brightness of the discharge as a whole: e.g. at 1 mm. Hg. pressure it was easy to obtain a high power discharge and the He II lines 3203 and 2733 were 'long', but at 0.07 mm.Hg. when it was difficult to match the discharge to the oscillator and its total brightness was less, both those lines were 'short'. The He II line at 2511 A. appeared only in the constriction and only at pressure of less than 1 mm. Hg. and was very feeble. Plate 8 shows the 'long' and 'short' lines photographed in 2 hours running time ( $\approx$  7.2 secs.exposure) with a wide slit (0.05 mm) but different pressures and (unavoidably) for different power dissipations.

### (16.3) Impurities.

Since the traps were not very efficient at these pressures (12.3) there were always impurities (such as Hg) in the spectrum. There were Si lines too which must have been produced by sputtering of the glass since they were



9B



most intense in the constriction, where the bombardment would be most intense, and there was no silicone grease in the system. The 'raies ultimes' of boron, (2947.7, 2946.8) also presumably came from the (pyrex) glass. The three possible sources of carbon for the CII lines were the Apiezon grease on the winch of the valve, the charcoal in trap T<sub>3</sub>, and the Araldite which cemented the quartz window to the tube. The grease undoubtedly contributed something because the intensity of the carbon lines was diminished by immersing trap T<sub>4</sub> in liquid air and a deposit of grease formed on the sides of the trap. When the discharge was running there was also a faint blue glow round the 'Araldite'. Fortunately, none of these lines fell near enough to any of the He lines to interfere with their contours. The lines of the heavier elements (Hg and Si) were indeed useful as 'norms' to show the broadening which had been caused by the instrument rather than by Doppler or Stark effect.

There was an unidentified line which fell at 2733.17A., within the contour of the He II line at 2733.32A. and was discovered from the asymmetry which it caused in the contour (shown in 9A). Its wavelength showed that it may have been a faint line of Xe II (2733.15) or A (2733.06) but its identity is doubtful because other lines of the same elements, which should have been much more intense, were not in the spectrum.

In nearly every spectrum taken of any of the r.f.

discharge tubes (5A, B, C, D.) there appeared to be a faint, complicated, system of bands extending from 3073A. to the red. These have not been identified, but the radicals probably came either from the tap-grease or from the 'Araldite'. There did not appear to be any He<sub>2</sub> band-heads at 3200.6 or 3206.4 A.U., nor any continuum (recombination spectrum).

(16.4) Use of lines of Hg. and Si as 'Norms'.

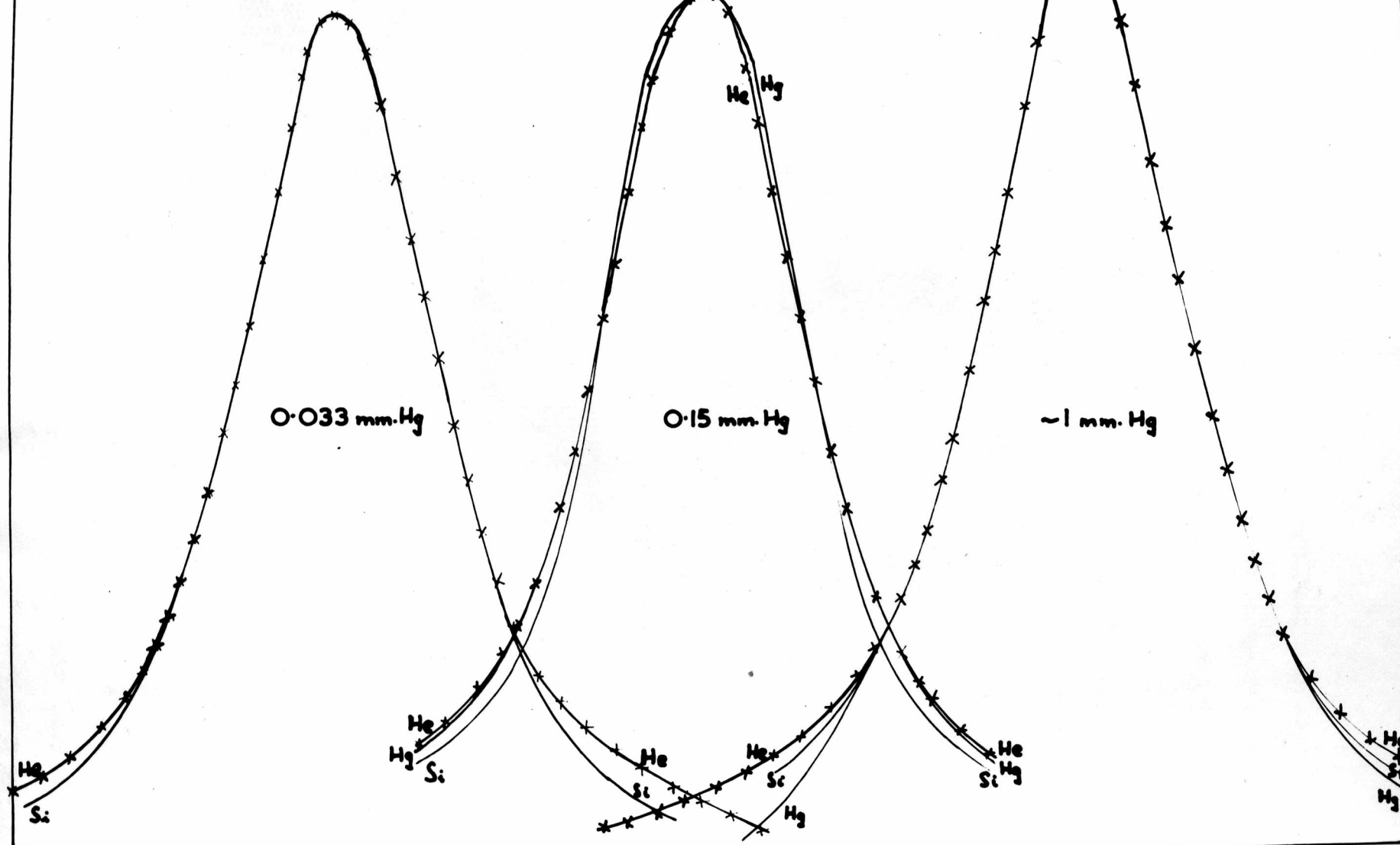
Lines of Hg and Si, the heaviest elements present in the spectra, were used to show the instrumental breadth alone since their respective Doppler breadths would be only  $(4/200)^{\frac{1}{2}}$  and  $(4/28)^{\frac{1}{2}}$  that of He. The maximum Doppler breadth  $b$  of the He lines was expected to be about equal to the instrumental breadth  $b_1$  and their resultant breadth  $b_2$  to be given by equation 13E:

$$\text{for He: } b_2^2 = b^2 + b_1^2 = 2 b_1^2 \text{ (approx.) (16A)}$$

$$\begin{aligned} \text{Similarly for Hg: } b_2^2 &= (b^2/50)_{\text{He}} + b_1^2 = (1 + 1/50) b_1^2 \\ &\quad \text{(approx.)} \\ \text{" " Si: } b_2^2 &= (b^2/7)_{\text{He}} + b_1^2 = (1 + 1/7) b_1^2 \\ &\quad \text{(approx.)} \end{aligned} \quad \left. \vphantom{\begin{aligned} \text{Similarly for Hg: } \\ \text{" " Si: } \end{aligned}} \right\} \text{(16B)}$$

Preliminary experiments (13.4) had shown the random error in the measurement of  $b_1$  to be  $\pm 20\%$ , so no further comparable error was introduced by assuming  $b_2^2 = b_1^2$  for both Hg and Si, and this was confirmed by later measurements not showing more than 20% difference between the breadths of their lines (table 5). Again,

10 He 2764 A  
(slit: 0.01 mm.)



0.033 mm.Hg

0.15 mm.Hg

~1 mm.Hg

He  
Si

He  
H<sub>2</sub>  
Si

He  
Si

He  
Si  
H<sub>2</sub>

He  
Si  
H<sub>2</sub>

He  
Si  
H<sub>2</sub>

no further error was introduced by measuring these 'norms' in a different region of the spectrum from that of the He lines, since previous measurements had not detected any variation of  $b_1$  with wavelength (13.4 and 9B), and this was also confirmed by later measurements (table 5). If more accurate measurements had been possible the equations of (16B) would have been a better approximation, and the preliminary experiments would have shown the variation of  $b_1$ , with wavelength.

The lines used as 'norms' were those of Hg at 2848 A. and of Si at 2882A.; other lines of Hg, which were nearer the He lines, were too faint to be used.

(16.5) The line contours.

The contours of the He lines at 2764 and 2829A. were compared with those of the 'norms'. The 'norms' were approximately Gaussian, as expected from (13.7), but the He lines were broader in the wings, as shown in (10). A more sensitive test (16.9) showed that both He and 'norms' contours deviated considerably from Gaussian ones, and that for the He lines it was probably caused by the combined effects of Stark broadening and the temperature drift of the spectrograph while for the norms it was caused by temperature drift alone. The He I line at 2723A. and the He II line at 2733A. were rather faint and their wing contours were lost in the background of the photograph, so it was not possible

TABLE 4.            THE SPECTRA.

<u>Symbol</u>	<u>Slit width (m.m.)</u>	<u>Pressure (mm. Hg.)</u>	<u>Temperature drift (°C) shown by:</u>	
			<u>thermometer</u>	<u>neon bulb spectrum</u>
S1	0.010	approx. 1	0.1	0.7
S2	0.010	0.15	0.2	1.2
S3	0.015	0.033	0.2	0.7
S4	0.010	0.033	0.1	1.05
S5	0.005	0.033	0.05	0.75

to compare them.

(16.6) Spectra used for the estimation of temperature.

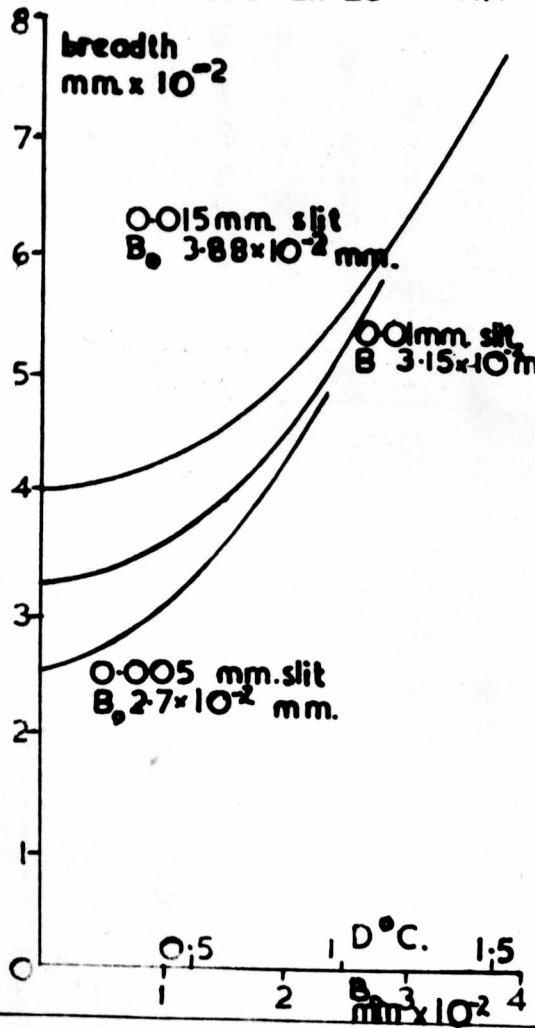
Only one photograph (7/4) proved finally to be useful for the estimation of the various temperatures, although another (7/3) would have been if the temperature drift of the spectrograph during the exposure had been indicated reliably by the thermometer on the spectrograph (discussed in 16.7).

Three spectra were taken with the same spectrograph slit width but at different pressures in order to show if there were Stark broadening at pressures above the minimum. Three spectra were taken at the minimum pressure but for different slit widths in order to show up any unforeseen instrumental effects. It is however probable that there was another variable, the power input, since the development of the tubes had not advanced sufficiently for this to be measured each time (12.5); in particular, the power input probably increased with pressure because it became easier to match the tube to the oscillator. Table 4 shows the experimental conditions: the two groups of three spectra each are S1, S2, S4 and S3, S4, S5. In S5 the lines at 2723 and 2733A were too faint for use; but the line at 2829A could be used because, in this spectrum alone, its peak intensity lay on the calibration curve (7B).

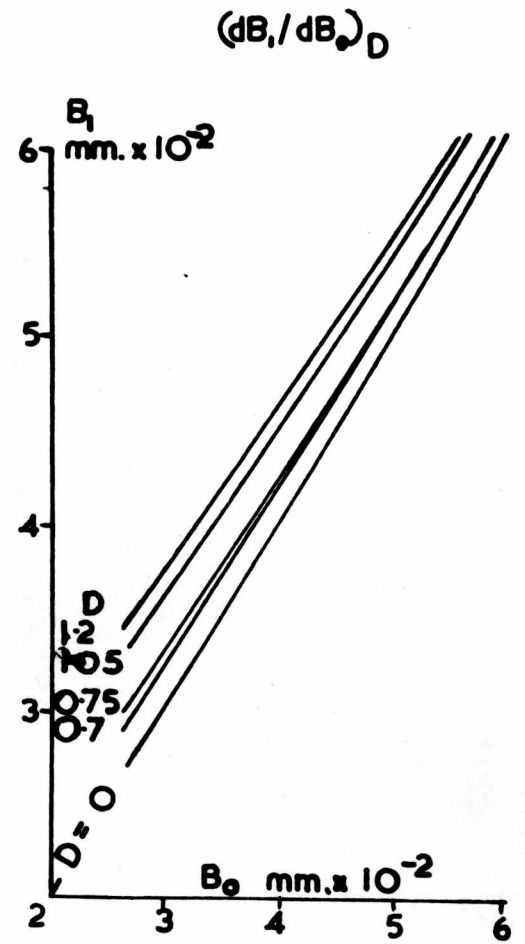
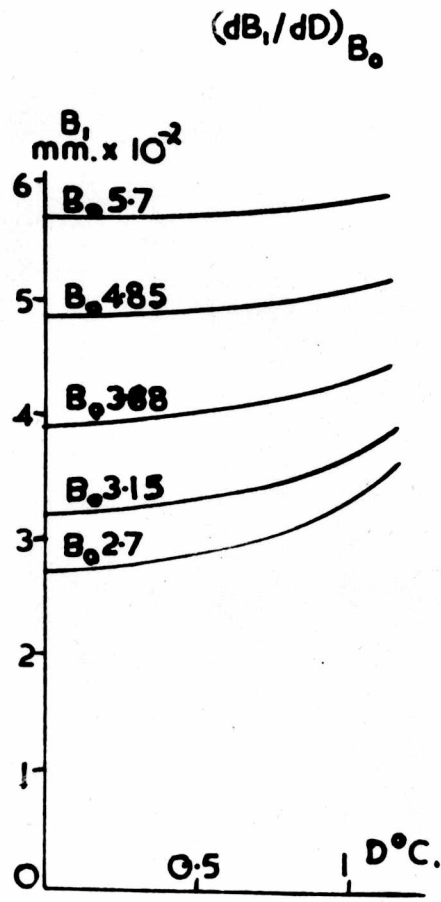
(16.7) Measurements of temperature drift made with the neon bulb spectrum.

On plate 7/3 the neon bulb spectra were overexposed and so could not be used. For plate 7/4 they

NEON BULB LINES IIA



HELIUM LINES AND 'NORMS' IIB & IIC



showed that temperature drift had been much larger than had been indicated by the thermometer attached to the spectrograph. The 'neon bulb' line measured was that of a mercury impurity at 3126A. and fell within the background of irregular band spectrum so the 'clear glass' reading of the microphotometer which was used was the average in the neighbourhood of the line. The contour of this line was the resultant of two instrumental contours whose breadth was determined by the width of the spectrograph slit and the separation of whose peaks was determined by the temperature drift during the exposure of the helium discharge. The variation of the breadth of the resultant with the separation  $X$  of the peaks of the components, was found graphically from the known instrumental breadths for the slit widths used, and is shown in 11A up to values of  $X$  for which the components become resolved. From these curves and the measured line breadths, the separation  $X$  was found and converted to temperature-drift from the results of (13.2). It corresponded to a much greater temperature-drift than had been shown by the thermometer on the spectrograph, (table 4). Evidently the spectrograph was not in thermal equilibrium through its entire volume of quartz, metal, and air.

(16.8) Correction of line breadths for the effect of temperature drift.

Let  $B_0$  be the breadth which any line would have had if there had been no temperature drift: for  $H_e$  lines

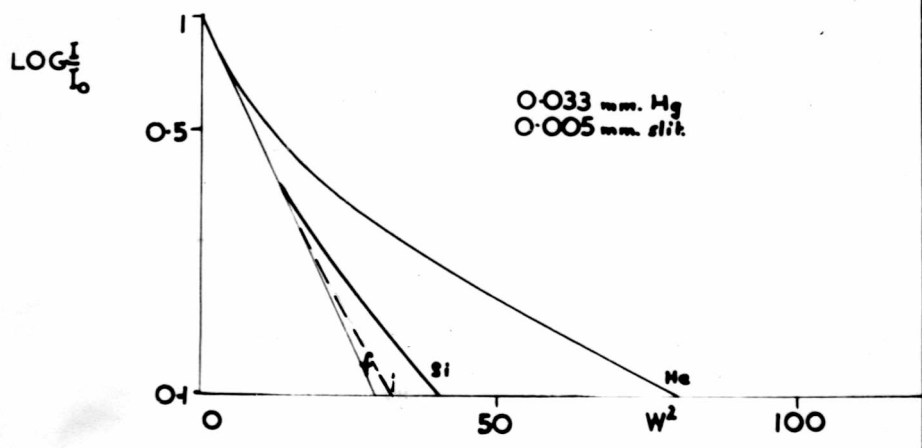
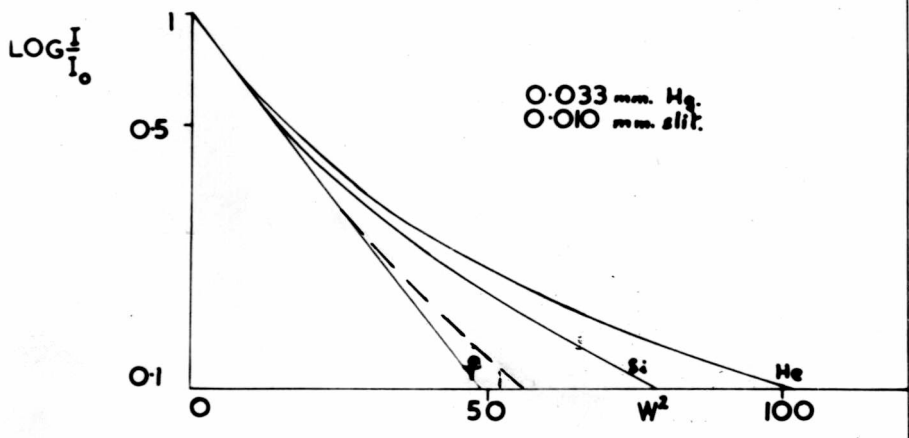
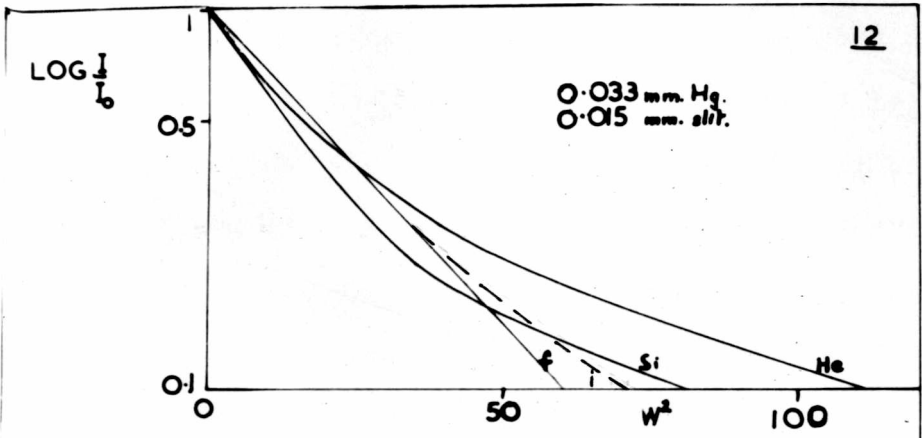
TABLE 5.  $B_1$  and  $B_0$  in units of 0.01 mm.

Spectrum		Norms			He II	He I		
		Hg 2848	Si 2882	Mean	2733	2723	2764	2829
<u><math>B_1</math></u>	S1	3.1	3.0		6.0	4.9	4.3	-
	S2	3.65	3.6		5.65	4.65	4.3	-
	S4	3.8	3.65		5.5	4.05	4.0	-
	S3	-	3.8		5.15	4.4	4.1	-
	S4	3.8	3.65		5.5	4.05	4.0	-
	S5	-	2.9		-	-	3.5	3.55
	S1	2.85	2.75	2.8	5.8	4.7	4.1	-
	S2	2.85	2.75	2.8	5.15	3.95	3.6	-
	S4	3.25	3.05	3.15	5.05	3.55	3.45	-
	S3	-	3.6	3.6	4.95	4.2	3.9	-
S4	3.25	3.05	3.15	5.05	3.55	3.45	-	
S5	-	2.6	2.6	-	-	3.25	3.3	

$B_0 = b_2$  of equation (13E), for the 'norms'  $B_0 = b_1$  (approx.) (16.4). The result of temperature drift  $D$  (found from neon bulb spectrum) would be to increase the observed breadth from  $B_0$  to  $B_1$ ; because the observed line contour of breadth  $B_1$ , would be the resultant of many contours of breadth  $B_0$  spread over a distance  $X$  equal to the separation which  $D$  had caused between the peaks of the neon bulb lines (16.7). If the contours were Gaussian when  $D = 0$ , and if there had been a uniform rate of drift, then it can be shown that the observed contours would be (Appendix 1):

$$I(x) = \left\{ \operatorname{erf} \frac{x}{(2s^2)^{\frac{1}{2}}} - \operatorname{erf} \frac{x-X}{(2s^2)^{\frac{1}{2}}} \right\} / 2KX \quad (16C)$$

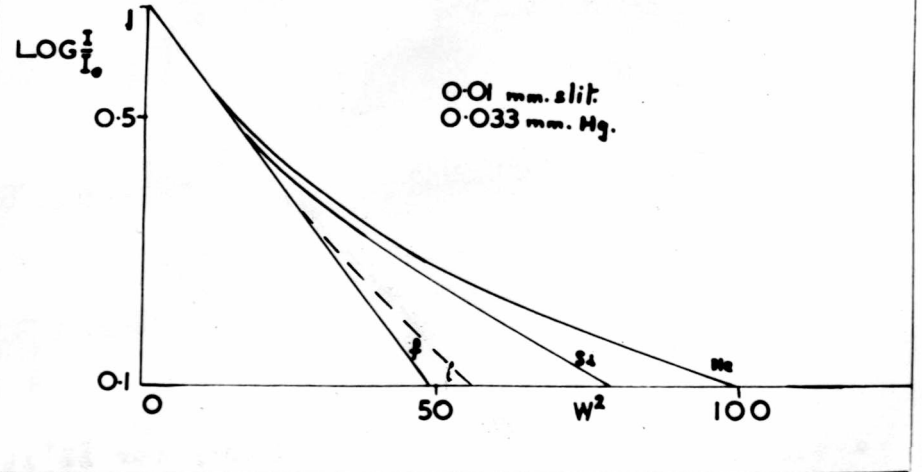
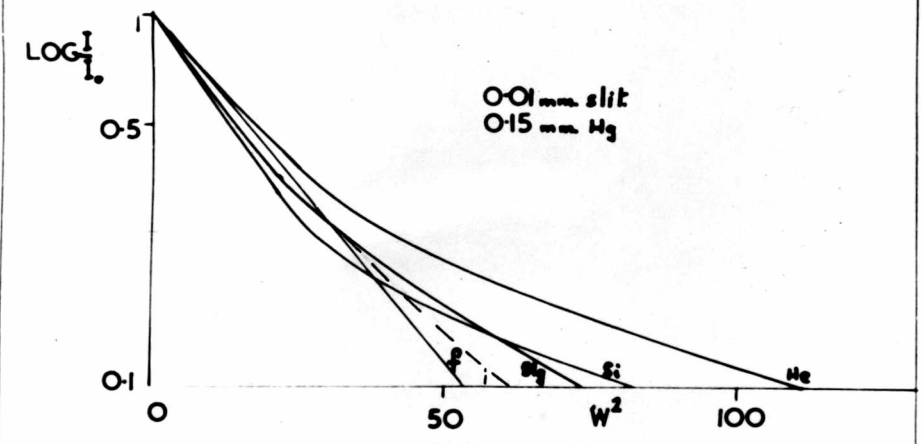
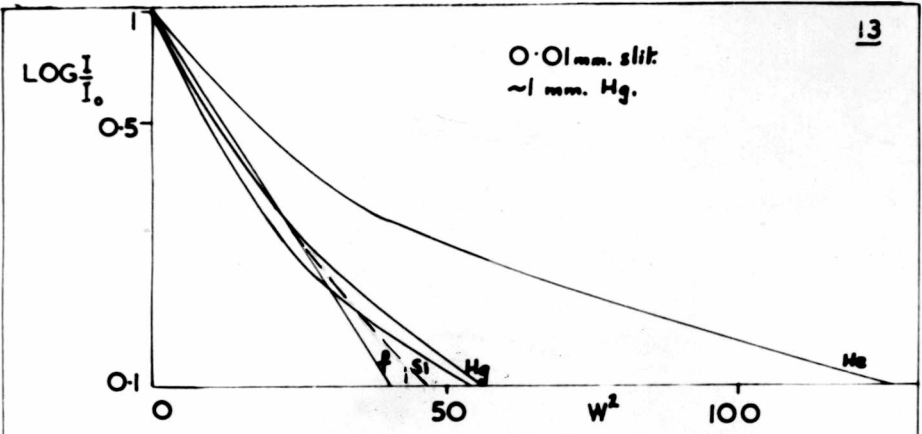
where  $I(x)$  is the intensity at  $x$ ,  $\operatorname{erf}$  is the error integral,  $s$  is the standard deviation,  $KX$  is the number of component contours of breadth  $B_0$ . From this equation a family of curves of  $(dB_1 / dD)_{B_0}$  was plotted for various values of  $B_0$ . These curves applied both to He and 'norm' lines since both were known to have approximately Gaussian contours when  $D = 0$  (13.7), and are shown in (11B). From these curves were deduced others of  $(dB_1/dB_0)_D$  for the values of  $D$  which had been found to apply to the spectra on plate 7/4 (16.7 and table 4). From the second set of curves (shown in 11C) the value of  $B_0$  for each line in each spectrum was found (table 5). The mean breadth  $B_0$  of the 'norms' for the three spectra which had been taken at the same slit width ( $S_1, S_2, S_4$ ) did not vary by much more than 10%; and for the



three spectra which had been taken at the same pressure but different slit widths, they agreed within about 10% with the instrumental line-breadths, (values of  $B_0$ , 2.6, 3.15,  $3.6 \times 10^{-2}$ mm.; instrumental breadths, 2.7, 3.1,  $4.0 \times 10^{-2}$ mm.). This shows that the assumptions of 16C were justified as a first approximation.

(16.9) Stark broadening of the Helium lines.

Table 5 shows that, for a given slit width,  $B_0$  for all the helium lines decreased with pressure, and that even at the lowest pressure it was considerably greater for the He II line at 2733A. than for the nearby He I line at 2723A. This indicates that even at the lowest pressure there was Stark broadening of the helium lines. It is confirmed by the shape of the contours (16.5), especially when tested by the more sensitive method of (13.7) which is to plot the logarithm of the intensity at any point against the square of the width of the contour. Such plots of  $\log(I/I_0)$  v.  $W^2$  are shown for various slit widths in (12) and for various pressures in (13); plots of typical instrumental contours (13.7) are labelled 'i', and plots of formula (16C) are labelled 'F'. The curves for the helium-line (2764A) show that: its deviation from the formula was always greater than that of the 'norms'; its deviation increased with pressure, but that of the 'norms' did not; and the deviation was greatest for the wings of the line (though that is exaggerated by the log scale of the graph). All this confirms that the helium lines suffered



from Stark broadening. The deviation of the plots for the 'norms' from those for the instrumental contours suggests that all the contours suffered from an irregular temperature drift, which emphasizes that (16C) is only a first approximation.

Since the broadening of the wings decreased with pressure and was less for He I than for He II, the effect of the constriction (discussed in 12.5) was evidently far less than Stark effect..

(16.10) The intensities of the helium lines.

Dr.J.D.Craggs suggested that the excitation temperature (7.4) and equilibrium temperature (7.5) might be estimated from the spectra which the author had already photographed before he left Birmingham. In order to do this the relative intensities of the helium lines were measured for the two groups of spectra  $S_1, S_2, S_4$  and  $S_3, S_4, S_5$  (16.6). In the previous measurements the variation of the breadth of each line ( $l_1, l_2 \dots \dots l_n$ ) with pressure had been studied in order to detect interference from Stark broadening, and in order to reduce the effect of any microphotometer zero-drift the contours had been plotted in the following order:-

- (i) that of  $l_1$  in  $S_1$ , then of  $l_1$  in  $S_2$ , then of  $l_1$  in  $S_4$ ,
- (ii) repeated for  $l_2$  in  $S_1, S_2, S_4$ ,
- (n) and so on up to  $l_n$  in  $S_1, S_2, S_4$ .

The same method had been used for the group  $S_3, S_4, S_5$ . However, the calculation of excitation and equilibrium

TABLE 6 Galvanometer Readings.

Average for clear glass = 24.0.

Spectrum	Wavelength (A)	(i)	(ii)	(iii)	(iv)	Mean
S1	2723	18.9	18.7	18.7	18.6	18.73
	2733	-	-	-	-	-
	2764	10.1	9.9	9.9	9.85	9.94
	2829	3.8	3.8	3.85	3.9	3.84
	2945	0.9	1.0	1.0	1.0	0.98
	3203	12.8	12.5	12.35	12.75	12.60
S2	2723	17.0	17.0	16.75	16.7	12.86
	2733	18.55	18.05	18.2	18.15	18.24
	2764	7.65	7.4	7.4	7.7	7.54
	2829	2.4	2.4	2.4	2.55	2.44
	2945	0.6	0.6	0.6	0.55	0.59
	3203	4.9	4.85	5.0	4.9	4.91
S4	2723	18.95	19.15	18.8	18.9	18.95
	2733	19.55	19.3	18.95	19.0	19.20
	2764	9.9	10.0	10.0	10.1	10.00
	2829	3.4	3.2	3.25	3.1	3.24
	2945	0.85	0.85	0.8	0.85	0.84
	3203	5.9	5.9	6.3	6.15	6.06
*****						
S3	2764	13.7	14.1	14.15	13.9	13.96
	2829	4.45	4.5	4.5	4.5	4.49
	2945	1.15	1.1	1.25	1.25	1.19
	3203	9.4	9.3	9.6	9.6	9.48
S4	2764	9.75	9.85	10.2	9.95	9.94
	2829	3.35	3.35	3.25	3.45	3.33
	2945	0.85	0.9	0.9	0.75	0.85
	3203	5.8	5.85	5.9	6.1	5.91
S5	2764	10.55	10.25	10.75	10.4	10.49
	2829	3.4	3.3	3.25	3.4	3.34
	2945	0.8	0.85	0.8	0.8	0.81
	3203	5.65	5.75	5.7	5.85	5.74

\*\*\*\*\*

temperatures depended on the relative intensities of  $l_1$ ,  $l_2$  . . . .  $l_n$  all at the same pressure, so even a slight zero drift during the previous measurements could have led to a systematic error if they had been used in the new calculations. The peak intensities of the lines were therefore measured anew in an order which was designed to reduce this error to a minimum:

- (i) scanned from  $l_1$  to  $l_n$  in  $S_1$  then in  $S_2$ , then in  $S_4$ ,
- (ii) repeated in the order  $S_4$ ,  $S_2$ ,  $S_1$ ,
- (iii) scanned from  $l_n$  to  $l_1$  in  $S_1$ , then in  $S_2$ , then in  $S_4$ ,
- (iv) repeated in the order  $S_4$ ,  $S_2$ ,  $S_1$ .

The same method was used for the group  $S_3$ ,  $S_4$ ,  $S_5$ . It was easy to ensure that the measured intensities referred to the same part of each line because the same slight irregularity of the spectrograph slit showed up on each one. The microphotometer was used with the same width and length of photocell slit as in the previous measurements. New calibration curves were plotted because for these new measurements the author used a microphotometer belonging to the British Aluminium Co., by courtesy of the Director of Research. The galvanometer deflections are shown in table 6, where (i) to (iv) refer to the four series of measurements. The most accurately measured intensities were those of the line at 2764A. since they always corresponded to fairly large galvanometer deflections and to the central portion of the calibration curve; so the relative intensities were normalized by taking that of

TABLE 7.

<u>Spectrum</u>	<u>Relative</u>			
	<u>S1</u>	<u>S2</u>	<u>S4</u>	<u>S1</u>
<u>HeI</u>				
2723	2.33	3.23	2.23	25.1
2764	9.25	14.4	9.45	100
2829	35.0	57.0	41.9	378
2945	148	245	172	1600
<u>HeII</u>				
2733	4.1	2.43	2.10	4.10
3203	5.9	26.0	19.7	64

<u>Spectrum</u>	<u>Relative</u>			
	<u>S3</u>	<u>S4</u>	<u>S5</u>	<u>S3</u>
2764	8.4	9.3	5.1	100
2829	39.9	41.0	29.5	475
2945	178	169	114	2120
3203	20.8	20.0	10.0	247

Intensities of helium lines.

Normalized		Mean	Differences from mean		
S2	S4	S	(S-S1)	(s-S2)	(s-S4)
22.4	23.6	23.7	-6%	6%	1%
100	100	100	-	-	-
3396	444	405	7%	2%	-10%
1700	1820	1710	6%	1%	-6%
16.8	22.1	16	38%	5%	-38%
180	208	151	58%	19%	-38%

Normalized			
S4	S5	% s.d.	Mean
100	100	-	100
440	575	15%	495
1820	2240	12%	2060
250	197	13%	220

2764A. as 100 units. Table 7 shows the relative intensities, the normalized intensities and the difference of the latter from the mean. The results for  $S_3$ ,  $S_4$ ,  $S_5$  (spectra for same pressure but different slit widths) show that for individual spectra the measurements had a standard deviation of 12% to 15%, and that although the measurements for  $S_1$ ,  $S_2$ ,  $S_4$  (same slit width, different pressures) showed there was a real increase in the relative intensity of the He II lines as the pressure decreased, they were not accurate enough to show whether there was a real change in the intensity of the He I lines. The rather large standard deviation was probably caused by the variation of unmeasured factors in the condition of the discharge, e.g. the power input.

TABLE 8. Corrected line-breadths,  $B_0$ , in  $\text{cm.}^{-1}$

Spectrum	Norms			HeII	He I		
	Hg.2848	Si 2882	Mean	2733	2723	2764	2829
S1	1.45	1.42	1.435	2.82	2.27	2.00	-
S2	1.44	1.42	1.43	2.51	1.91	1.75	-
S4	1.63	1.56	1.595	2.46	1.71	1.68	-
S3	-	1.83	1.83	2.40	2.02	1.90	-
S4	1.63	1.56	1.595	2.46	1.71	1.68	-
S5	-	1.34	1.34	-	-	1.58	1.67

\*\*\*\*\*

TABLE 9. Apparent temperature in  $^{\circ}\text{K}$ , calculated from line breadths

Spectrum	He II	He I		
	2733	2723	2764	2829
S1	34,000	18,000	11,500	-
S2	25,000	9,000	6,000	-
S4	20,000	2,300	1,700	-
S3	14,000	4,200	1,600	-
S4	20,000	2,300	1,700	-
S5	-	-	4,200	6,000

\*\*\*\*\*

17. RESULTS AND DISCUSSION.(17.1) Gas temperature, deduced from line-breadths.

The corrected line breadths,  $B_0$  (16.8), were converted to  $\text{cm}^{-1}$  (table 8) and the square of the Doppler breadth of the helium lines,  $b^2$ , was deduced from equation (13E):

$$b^2 = b_2^2 - b_1^2 \quad (17A)$$

where, in terms of  $B_0$ :  $b_2$  equals  $B_0$  for the helium lines, and  $b_1$  equals the mean of  $B_0$  for the 'norms'. The gas temperatures,  $T$ , were deduced from the equation (8A):

$$T = 7.8 \times 10^{12} (b^2/n^2) \quad (17B)$$

where  $n$  is the wavenumber of the appropriate line. They are shown in table 9.

The random errors  $db_1$  in  $b_1$  and  $db_2$  in  $b_2$  had each been estimated as 20% (13.4., 16.4) so the random error  $dT$  in  $T$  would be 80% since:

$$dT = 2 db = 2(db_1 + db_2) \quad (17C)$$

This agreed with the standard deviation of the results.

For the six values of  $T$  deduced from the He I lines in the three spectra  $S_3$   $S_4$   $S_5$  which had been taken at the same pressure, it was about 60% (s.d.  $2100^\circ\text{K}$  and mean  $T$   $3350^\circ\text{K}$ ), so for the two values of  $T$  deduced from any one spectrum it was  $(6/2)^{\frac{1}{2}}$  times as great and the values of  $T$  were only reliable to about a factor of two.

The apparently greater temperature of the He II ions compared with He I atoms at all pressures in attributable to the greater sensitivity of the ions to

Stark broadening; and the apparent decrease of the temperature of both ions and atoms with pressure is attributable to the decrease of Stark effect with pressure. Such interference from Stark effect would mean that the values of  $T$  were only upper limits, and their low value would be owing to the practical difficulty of getting high power into a low-pressure discharge, and possibly to the effect of the constriction (12.5).

Another possible explanation of these effects is that emission of He I lines may have continued in the afterglow, and therefore  $T$  would have been only an average temperature over the whole period of discharge and afterglow, and decreased at lower pressures as the afterglow persisted for longer periods. These He I lines, generally accompanied by He<sub>2</sub> bands, can be produced in afterglows by dissociative recombination (Massey, 1952) in which the molecular ion He<sub>2</sub><sup>+</sup> first combines with an electron to form He<sub>2</sub> and then dissociates into 2 H<sub>e</sub>. Such lines would have been expected to be most intense at the centre of the constriction because the rate of all types of volume recombination is proportional to the product of the electron and ion concentrations and these concentrations are greatest at the centre. No such enhancement of the centres of the He I lines could be detected, nor could any band heads of He<sub>2</sub>, so it seems that the afterglow contribution was small; however, this effect cannot be entirely excluded in the absence of direct experimental knowledge of the afterglow spectrum of

TABLE 10.  
Apparent Excitation Temperatures.

<u>Spectrum on plate</u>	<u>Spectral series</u>	<u>Lines compared</u>	<u>T<sub>x</sub> in °K.</u>	
(mean)	He I	2945 & 2723A.	1350	} (a)
		2829       "	1000	
		2764       "	750	
"	"	2945 & 2829A.	2100	} (b)
		"       2764A.	1700	
		"       2723A.	1350	
"	"	2945 & 2829A.	2100	} (c)
		2829 & 2764A.	1250	
		2764 & 2723A.	750	
S2	He II	3203 & 2733A.	4100	
S4	"	"       "	4400	

the particular discharge since recent work with high-power (un-constricted) r.f. discharges in helium has shown that the He I spectrum may last for many micro-seconds (Janin and Eyraud, 1953; Bryant, 1955, private communication).

### (17.2) Excitation Temperature.

The excitation temperature  $T_x$  was calculated from the relative intensities of the He II lines at two pressures (line 2723A was too faint at the highest pressure) and from the mean relative intensities of the He I lines (table 7), using the equation:

$$T_x = C_1 / \log \left\{ \frac{I_{nr}}{I_{nr}} \cdot C_2 \right\} \quad (17D)$$

This equation is derived in Appendix 2:  $I_{nr}$  and  $I_{nr}$  are the relative intensities of two lines in the same spectral series, and  $I_{nr}$  corresponds to the line of shorter wavelength;  $C_1$  and  $C_2$  are constant for a given pair of lines. The results are shown in table 10. For He II the higher value of  $T_x$  was for the lower pressure, which was to be expected since the electrons then had a greater chance of reaching a high energy. However, there were three ways in which the results were unexpected:  $T_x$  was not the same for each pair of lines, was not the same for He I and He II, and was not of the order of magnitude of the probable electron temperature (c.50,000°K. at these pressures). It is unlikely that any of these anomalies were caused by the transmission of the spectrograph or the spectral

response of the emulsion, since both these would have caused a decrease of sensitivity with wavelength. This decrease of sensitivity would have caused most reduction in intensity for the lines of shortest wavelength and therefore the values of  $T_{ex}$  calculated from (17D) would have been least for lines which were furthest apart: but this does not agree with groups (a) and (c) of table 10.

The most likely reason for the anomalies is that the collisions of the electrons with the walls of the constriction changed their velocity distribution from the Maxwellian one assumed in 17D. The proportion of high energy electrons would be decreased and the proportion of low energy ones increased, both because of inelastic collisions with the walls and because of secondary electron emission from the walls. The higher the excitation potential of a spectrum line, the more its intensity would be decreased because of the lower proportion of high-energy electrons. The change in the relative intensity of two lines would be in the sense of weakening the one of shorter wavelength, and this would be most marked when both were of short wavelength. Consequently  $T_x$  calculated from (17D) would be too low, and would appear to be least when deduced from the two lines of shortest wavelength. This agrees with the experimental results, as is shown by comparing them in groups (a) (b) (c) of table 10. The explanation is not entirely satisfactory for the He II lines, since although ordinary Saha equation (Appendix 3), as shown in table 11B,

one was of long wavelength, yet obviously both had a higher excitation potential than any of the He I lines and so the calculated value of  $T_x$  would have been expected to be lower.

In view of this, the possibility of some contribution from the afterglow cannot be excluded, for this also would reduce the value of  $T_x$ , and would not have so much effect on He II as on He I lines because the number of excited ions would be reduced by recombination as well as by de-exciting collisions and by diffusion.

### (17.3) Equilibrium Temperature.

The equilibrium temperature  $T_s$  was estimated by comparing the intensities of the He II lines with the mean intensities of the He I lines (table 7), using the equation:

$$\log T_s - \frac{C_3}{T_s} = \frac{2}{5} \log \left\{ \frac{I_i}{I_a} \cdot N_e \cdot C_4 \right\} \quad (17E)$$

This equation is derived in Appendix 3:  $I_i/I_a$  is the ratio of the intensity of an ionized line to that of an atomic line;  $C_3$  and  $C_4$  are constants for a given pair of lines;  $N_e$  is the electron concentration, and its value was chosen so as to make the results internally consistent. It follows from (17.2) that the most reliable values of  $I_i$  and  $I_a$  were likely to be those for the lines of longest wavelength. The value of  $N_e$  was therefore chosen so that  $T_s$  calculated from  $I_i$  for 3203A. and  $I_a$  for 2945A., gave the correct percentage of ionization when it was put in the ordinary Saha equation (Appendix 3), as shown in table 11B.

TABLE 11. Apparent equilibrium temperature.

<u>Spectrum on plate</u>	<u>Lines compared</u>	<u>T<sub>s</sub> in °K.</u>	<u>Lines compared</u>	<u>T<sub>s</sub> in °K.</u>
S1	3203 & 2945 A.	16,300		
	" 2829A.	16,900		
	" 2764 A.	17,600		
	" 2723 A.	18,600		
S2	3203 & 2945 A.	15,900	2733 & 2945 A.	15,100
	" 2829 A.	16,500	" 2829 A.	15,600
	" 2764 A.	17,100	" 2764 A.	16,100
	" 2723 A.	18,000	" 2723 A.	16,800
S4	3203 & 2945 A.	15,100	2733 & 2945 A.	14,400
	2829 A.	15,600	" 2829 A.	14,800
	2764 A.	16,100	" 2764 A.	15,300
	2723 A.	16,900	" 2723 A.	16,000

TABLE 11B. % ionization, assumed and calculated

<u>Spectrum on plate:</u>	<u>S1</u>	<u>S2</u>	<u>S4</u>
Pressure in mm. Hg.	1	0.15	0.033
T <sub>s</sub> , from 3203 & 2945 A.	16,300	15,900	15,100
No. of atoms / cc.	3.56 x 10 <sup>16</sup>	5.34 x 10 <sup>15</sup>	1.07 x 10 <sup>15</sup>
No. of ions / cc. assumed:	1.5 x 10 <sup>16</sup>	3.5 x 10 <sup>15</sup>	0.8 x 10 <sup>15</sup>
% ionization assumed:	42%	66%	75%
% ionization at T <sub>s</sub> :	43%	66%	78%

The results are shown in table 11. They are consistent with the assumption made in (17.2) that the effect of the constriction would be to decrease the intensity more for the shorter wavelength lines than for the longer wavelength ones.  $T_S$  is a function of  $(I_i/I_a)$ ; the results show that values of  $T_S$  derived from  $I_i$  for 2723A. are lower than those derived from  $I_i$  for 3203A.; also, that for a given He II line ( $I_i$ ),  $T_S$  is greatest for the shortest He I line (least  $I_a$ ).

At the low pressures used,  $T_S$  would not correspond either to the gas temperature  $T_g$  or to the electron temperature  $T_e$ . The results for  $T_S$  mean that if the ionization had been produced by collisions between atoms having a Maxwellian distribution of energies (as assumed in Saha's equation from which 17E is derived), then that energy distribution would correspond to a temperature of the order of 16,000°K. However, in the low-pressure discharges which were used, the ionization would be produced by electron impact, so  $T_e$  would be much greater than  $T_S$  and  $T_g$  would be much less. The results for  $T_S$  are only an indication of its order of magnitude, because of the complications caused by the constriction in the tube and by the afterglow. Nevertheless they afford further evidence for conclusions reached in (17.2) and (17.1) respectively: that the apparent excitation temperatures were far too low to correspond to the electron temperature; and that the breadths of the He II lines were too great to correspond to the gas temperature.

18. SUGGESTIONS FOR FUTURE WORK.

(18.1) Work with the present apparatus.

It is considered unlikely that much improvement in the measurement of gas temperature from the Doppler broadening of the spectrum lines can be made with the present apparatus.

However, this apparatus could be used to measure excitation temperatures of r.f. discharges, and by using a rotating sectored disc between the discharge and the spectrograph it would be possible to compare the excitation temperature of the discharge and its afterglow. It would be advantageous to use spectrum lines in the visible region, because for that region: the transmission of the seven-step filter is known, the transmission of the spectrograph and the response of the photographic plate could be found by using a standard tungsten-filament lamp and exposure times would be shorter.

(18.2) Work with additional apparatus.

The present work has shown that any future measurements of the Doppler broadening of spectrum lines from an r.f. discharge would need to be carried out at pressures of the order of 0.01 mm. Hg. in order to avoid Stark broadening, using a gas-circulating system to overcome losses from 'clean-up' and constricted discharge tube in order to concentrate the power into a small volume of gas. It would also be advisable to measure the power input to the discharge, to match the discharge to the oscillator, and to avoid

photographing the afterglow spectrum. It would be best to study the spectra with a Fabry Perot interferometer, because of the comparative ease with which the temperature of its small volume could be controlled and because of its great dispersion. Its dispersion would enable lines in the visible region to be used and these would be of greater Doppler breadth and higher intensity than those in the ultra-violet; also, the experiment would not have to be restricted to the lightest elements.

lines. Assuming that the temperature is uniform, the contour of the lines could be:

$$I(x) = \frac{1}{N\lambda} \int_0^{\infty} \exp\left\{-\frac{(x-y)^2}{2s^2}\right\} dy$$

where values of I are normalized by dividing them by the number of components Nλ, (this is proportional to λ).

Substituting  $z^2 = (x - y)^2 / 2s^2$

$$I(x) = \frac{1}{N\lambda} \cdot \frac{2}{\pi^{1/2}} \int_0^{\infty} \frac{\exp(-z^2) dz}{x/(2s^2)^{1/2}}$$

$$= \frac{1}{N\lambda} \left\{ \operatorname{erf} \frac{x}{(2s^2)^{1/2}} - \operatorname{erf} \frac{(x - Y)}{(2s^2)^{1/2}} \right\}$$

where 'erf' is the 'probability integral' and is tabulated; negative values of 'erf' are not tabulated but  $\operatorname{erf}(-z) = -\operatorname{erf}(z)$ . The author thanks R.V.B. Taylor of the Electron Physics Department for this mathematical analysis.

APPENDIX I.

EQUATION (16C)

The contour of each 'norms' is the resultant of many Gaussian curves: of standard deviation  $S$  for which it is

$$I(x) = (2\pi s^2)^{-\frac{1}{2}} \exp \left\{ - (x - p)^2 / 2s^2 \right\}$$

where  $p$  is the value of  $x$  at the peak of the curve.

These are spread out over a distance  $x$  equal to the separation between the peaks of the corresponding neon bulb lines. Assuming that the spreading due to temperature drift was uniform, the contour of the norm would be:

$$I(x) = \frac{1}{NX (2\pi s^2)^{\frac{1}{2}}} \int_0^X \exp \left\{ -(x-p)^2 / 2s^2 \right\}$$

where values of  $I$  are normalized by dividing them by the number of components  $NX$ , (this is proportional to  $X$ ).

$$\text{Substituting } z^2 = (x - p)^2 / 2s^2$$

$$I(x) = \frac{1}{2NX} \cdot \frac{2}{\pi^{\frac{1}{2}}} \int_{x/(2s^2)^{\frac{1}{2}}}^{(x - X)/(2s^2)^{\frac{1}{2}}} \exp(-z^2) dz$$

$$= \frac{1}{2NX} \left\{ \operatorname{erf} \frac{x}{(2s^2)^{\frac{1}{2}}} - \operatorname{erf} \frac{(x - X)}{(2s^2)^{\frac{1}{2}}} \right\}$$

where 'erf' is the 'probability integral' and is tabulated; negative values of 'erf' are not tabulated but  $\operatorname{erf}(-z) = -\operatorname{erf}(z)$ . The author thanks Mr. J. B. Taylor of the Electron Physics Department for this mathematical analysis.

APPENDIX 2.

Equation (17D).

When an atom changes from an energy state whose excitation potential is  $V_n$  to a lower one for which it is  $V_r$ , it emits light of frequency  $f_{nr}$  and absolute intensity  $J_{nr}$  given by

$$hf_{nr} = eV_n - eV_r$$

and for a given  $J_{nr} = h \cdot f_{nr} A_{nr} N_n$

where  $h$  is Planck's constant,  $e$  is the electronic charge,  $A_{nr}$  is Einstein's A coefficient for spontaneous transition from state  $n$  to  $r$ ,  $N_n$  is the concentration of atoms in state  $n$ .  $N_n$  may be related to the concentration  $N_0$  in the ground state, the statistical weights  $g_0$  and  $g_n$  of the ground state and state  $n$ , and the excitation temperature  $T_x$ , by

$$N_n = N_0 (g_n/g_0) \exp(-eV_n/kT_x)$$

This relationship assumes that the concentration of atoms in the various energy states is determined by collisions with only one type of particle, that those particles have a Maxwellian energy distribution, and that none of the energy states has either a very long or a very short half life. With these conditions

$$J_{nr} = h \cdot f_{nr} A_{nr} N_0 (g_n/g_0) \exp(-eV_n/kT_x)$$

The equations are similar for a transition from a state whose excitation potential is  $V_m$ , so the relative intensity of lines of frequencies  $f_{mr}$  and  $f_{nr}$  is

$$\frac{I_{mr}}{I_{nr}} = \frac{J_{mr}}{J_{nr}} = \frac{f_{mr} A_{mr} g_m}{f_{nr} A_{nr} g_n} \exp. \left\{ \frac{eV_n - eV_m}{kT_x} \right\}$$

Equation (17D) Cont.....

Therefore  $T_x$  may be found from relative intensities (I) rather than from absolute ones (J)

$$T_x = \frac{(f_{nr} - f_{mr}) h/k}{\ln \left\{ (I_{mr} f_{nr} A_{nr} g_n) / (I_{nr} f_{mr} A_{mr} g_m) \right\}}$$

and for a given pair of lines this may be written in terms of constants  $C_1$  and  $C_2$

$$T_x = C_1 / \log \left\{ \frac{I_{mr}}{I_{nr}} C_2 \right\}$$

where the other symbols are defined as in Appendix 2. Consequently the intensity of radiation emitted by an atom changing from state  $n$  to state  $m$  is

$$J_n = (N_n/V_n) h \nu_{nr} A_{nr} g_n \exp(-eV_n/kT)$$

and by an ion changing from state  $n$  to state  $s$  is

$$J_s = (N_s/V_s) h \nu_{ns} A_{ns} g_s \exp(-eV_s/kT)$$

where  $V_n$  and  $V_s$  are the excitation potentials in e.s.u. Substituting for  $V_n$   $E_1/V_1$   $E_s/V_s$  from Fowler's equation and putting  $g_n = 2$

$$\frac{I_1}{I_s} = \frac{J_1}{J_s} = \frac{2 \cdot (2\pi m k)^{3/2} \cdot g_n E_{ns} A_{ns} \cdot T^{3/2} \exp\{-e(V_1 + V_n - V_m)/kT\}}{N_0 h^3 \cdot g_n f_{nr} A_{nr}}$$

for two given spectral lines, one of the ion and one of the atom,

$$\log T_x = \frac{C_3}{T_x} = \frac{2}{3} \log \left\{ \frac{I_1}{I_s} \cdot E_0 \cdot C_4 \right\}$$

where  $C_3$  and  $C_4$  are constants for a given pair of lines.

APPENDIX 3.

EQUATION (17B)

Saha's equation in terms of the percentage ionization  $x$ , pressure  $p$  in mm. Hg., ionization potential  $V_i$  in e.s.u., and absolute temperature  $T$  is

$$\log \left\{ \frac{px^2}{760(1-x^2)} \right\} = -\frac{(1.51 \times 10^6 \cdot V_i)}{T} + 2.5 - 2.5 \log T - 6.5$$

Fowler has shown that this may be written in terms of the concentrations of ions ( $N_i$ ), atoms ( $N_a$ ) and electrons ( $N_e$ ), and the partition functions  $V_i$  and  $V_a$  for ions and atoms, as

$$\frac{(N_i N_e)}{N_a} = \frac{(V_i/V_a)(g_e/h^3)(2\pi m kT)^{3/2} \exp(-eV_i/kT)}{1}$$

where the other symbols are the same as in Appendix 2.

Consequently the intensity of radiation emitted by an atom changing from state  $m$  to state  $r$  is

$$J_a = (N_a/V_a) h \cdot f_{mr} A_{mr} \epsilon_m \exp(-eV_m/kT)$$

and by an ion changing from state  $n$  to state  $s$  is

$$J_i = (N_i/V_i) h \cdot f_{ns} A_{ns} \epsilon_n \exp(-eV_n/kT)$$

where  $V_m$  and  $V_i$  are the excitation potentials in e.s.u.

Substituting for  $V_a N_i/V_i N_a$  from Fowler's equation and putting  $g_e = 2$

$$\frac{I_i}{I_a} = \frac{J_i}{J_a} = \frac{2 \cdot (2\pi mk)^{3/2}}{N_e h^3} \cdot \frac{\epsilon_n f_{ns} A_{ns}}{\epsilon_m f_{mr} A_{mr}} \cdot T^{3/2} \exp\left\{-e(V_i+V_n-V_m)/kT\right\}$$

So for two given spectrum lines, one of the ion and one of the atom,

$$\log T_s - \frac{C_3}{T_s} = \frac{2}{3} \log \left\{ \frac{I_i}{I_a} \frac{N_e}{T_s} C_4 \right\}$$

where  $C_3$  and  $C_4$  are constant for a given pair of lines.

#### APPENDIX 4.

##### Transition probabilities and statistical weights.

~~Babcock~~ The transition probabilities for He I were deduced from formulae given by Goldberg (1939). For He II they were deduced from values for the hydrogen atom given by Menzel and Perkeris (1935), since these are one sixteenth of the probability of transition between the corresponding states of the helium ion.

~~Edels~~ (The statistical weight of an energy state is  $(2j + 1)$  where  $j$  is the total angular momentum quantum number. The He I lines were for transitions from  $n^3P$  to  $2^3S$  states, and since for each  $n^3P$  state  $j$  could be 0, 1, or 2 their statistical weight  $g_n = 1 + 3 + 5 = 9$ . The He II lines were for transitions from the  $n^{\text{th}}$  to the third level of the ionized atom; for a one-electron atom  $(2j + 1) = n^2$ , therefore for the lines at 2733A. ( $n = 6$ ) and 3203A. ( $n = 5$ ) the statistical weights were 72 and 50.

Maecker (1951) *Zeit. f. Physik.* 136.119.

Massey (1952) *Advances in Physics.* 1.395.

Meinel (1950) *Phys. Rev.* 82. 1036.

Menzel & Perkeris (1935) *M.N.Roy. Astron.Soc.* 86.77.

Mitra (1947) 'The Upper Atmosphere', (R.A.S.B., Calcutta).

Mohler (1933) *Bur.Standards J.Res.* 10.771., 19.417 & 439.

Mohler (1942) *Inst.Phys.* 'Temperature'. (Reinhold).

Ornsfeld & Van Noy (1927) *Zeit.f.Physik.* 28.734.

REFERENCES FOR PART II.

- Allen (1932) Phys.Rev. 39. 46.
- Babcock (1923) Astrophys. Jnl. 57. 209.
- Biondi (1951) Phys. Rev. 82. 454.
- Churchill (1944) Ind. and Eng. Chem., Analytical Ed.16.653.
- Cillie (1936) Mon. Not. Roy. Ast. Soc. 96. 771.
- Craggs and Meek (1946) Proc. Roy. Soc. A.186. 241.
- Craggs and Hopwood (1947) Proc. Phys. Soc. 59. 755.
- Edels (1950) Brit. Elec. A.I.Res.Assoc. Report L/T 230.
- Edels & Craggs (1951) Proc.Phys.Soc. A.84. 562 and 574.
- Fabry and Buisson (1912) Comptes Rendus. 154. 1244.
- Foster (1953) Thesis. University of California (Berkeley).
- Gartlein (1951) Phys. Rev. 81. 463.
- Gaydon & Wolfhard (1949) Proc.Roy.Soc. A. 199. 89.
- Goldberg (1939) Astrophys. Jnl. 90. 414.
- Janin & Eyraud (1953) Comptes Rendus 237. 1073.
- Kruithof. (1943 & 4) Physica. 10.493 and 11.129.
- Maecker (1953) Zeit. f. Physik. 136.119.
- Massey (1952) Advances in Physics. 1.395.
- Meinel (1950) Phys. Rev. 80. 1096.
- Menzel & Perkeris (1935) M.N.Roy. Astron.Soc. 96.77.
- Mitra (1947 'The Upper Atmosphere'. (R.A.S.B., Calcutta).
- Mohler (1933,7) Bur.Standards J.Res. 10.771., 19.447 & 559.
- Mohler (1941) Am. Inst.Phys. 'Temperature'.(Reinhold).
- Ornstein & Van Wyk (1932) Zeit.f.Physik. 78.734.

References for Part II, Cont....

Ornstein & Minnaert (1927) Zeit.f.Physik. 43.404.

Ravenhill & Craggs (1951) Proc.Phys.Soc. B.64.618.

Redman (1954) Nature 174.247.

Saha (1950 'Treatise on Heat'. (Indian Press).

Schoen & Holmes (1954) J.Opt.Soc.Am. 44.502.

Suits (1941) Am.Inst.Phys. 'Temperature'. (Reinhold).

White (1934) 'Atomic Spectra'. (McGraw Hill).